The Function of Pap in the *Sinorhizobium meliloti* Pap-Pit Low Affinity Phosphate Transport System

By

Hui Zhao

September 24, 2013

A Thesis submitted to the School of Graduate Studies

for the Degree of Master of Science

McMaster University

The Function of Pap in the *S. meliloti* Pap-Pit Low Affinity Phosphate Transport System

MASTER OF SCIENCE (Biology 2013) McMaster University

Hamilton, Ontario

TITLE: The Function of Pap in the the *Sinorhizobium meliloti* Pap-Pit Low Affinity Phosphate Transport System

AUTHOR: Hui Zhao, B.Sc (Henan Agricultural University)

SUPERVISOR: Dr. T. M. Finan

ABSTRACT

Pap-Pit is a low affinity phosphate transporter found in *S. meliloti* and many other microorganisms. Pit is the transporter and Pap is the Pit accessory protein. Pap has been shown to be required for the function of Pap-Pit system in *S. meliloti*. In this study, *pap-pit* or *pit* alone from three species of bacteria have been expressed *in trans* in the *E. coli* Pi uptake mutants to check their ability to complement the Pi uptake deficiency of the hosts. A visualization tag, SNAP-tag, has been fused to *S. meliloti* Pap to help determine the subcellular localization of Pap. Here we show that there is an optimal level of Pap-Pit in the cells, and Pap appears to modulate this level to optimize the function of the system. We also demonstrate that Pap is probably localized intracellularly along the cell membrane. In addition, a *S. meliloti pap-pit* deletion strain has been prepared and to be used as the background strain for site-directed mutagenesis in Pap. The highly conserved surface amino acids in Pap have been identified to be the candidates for the mutagenesis.

ACKNOWLEDGEMENTS

I would like to thank Dr. Turlough Finan for giving me the opportunity to work and learn in his laboratory and for being such a helpful supervisor during the two years. I also appreciate the help and friendship from all the members of our laboratory and Barb, and many thanks to Dr. Kuroda for sharing with us his valuable strains and plasmids. I would like to say thank you and love you to my dear parents, Fumei Hui and Taishan Zhao, who may not know the differences between protein and DNA but always enjoy listening to me talking about my work. I would also like to thank my forever friends Xiaoya Wang, Huiyang Xiong and Youya Zhai for their support during my frustration and wish them good luck with their ongoing graduate work.

Table of Contents

LIST OF FIGURES

LIST OF TABLES

INTRODUCTION

Sinorhizobium melioti and phosphate uptake

S. meliloti is a Gram-negative alpha-proteobacterium. It has a 3.7kb chromosome and two megaplasmids, the 1.4kb pSymA and the 1.7kb pSymB. It interacts with its host plant, alfalfa, in a symbiotic relationship resulting in the formation of N_2 fixing nodules. This relationship allows the host plant to benefit from the reduced nitrogen fixed by the bacteroids in nodules and in return, the plant provides the bacteria with reduced carbon sources (Long 2001).

Phosphorous is an essential element in organisms. It is the most important component of the phospholipid bilayer and it also serves as a key constituent in nucleic acids, lipopolysaccharides, ATP and cofactors. In the natural environment, there are various phosphorous containing compounds to meet the requirements of bacteria for phosphorous. Among these compounds, inorganic phosphate (Pi) is the most favorable source of phosphorous for bacteria. Therefore, Pi uptake systems are of great importance to bacteria. *S. meliloti* has three different types of phosphate transporters. PstSCAB, PhnCDET and the Pap-Pit system. *S. meliloti* also has organophosphate transporters such as Ugp system for glycerol-3-phosphate.

Common Bacterial Transporters

The Major Facilitator Superfamily (MFS)

MFS is one of the most important transport superfamilies in bacteria. About 25%

of known transporters in bacteria are members of this superfamily (Law, Maloney et al. 2008). MFS members can transport a variety of substrates including ions, sugars, phosphates, drugs, nucleosides, amino acids, and peptides (Law, Maloney et al. 2008). Transporters of MFS are secondary transporters which uses electrochemical gradient as the energy source as opposed to primary transporters which hydrolyze ATP for energy.

Almost all major facilitator carriers consist of twelve transmembrane α-helices (TMs) which are connected by hydrophilic loops (Pao, Paulsen et al. 1998, Saier, Beatty et al. 1999). Most MFS proteins function as monomers. The MFS protein must transport a particular type of ion down its concentration gradient across the membrane to provide energy for the transport of the target substance against its concentration gradient. The direction of the transport of the two substance can be the same (symporter) or opposite (antiporter) (Saier, Beatty et al. 1999).

The transport of the substrate across the membrane is achieved by conformational changes that occur during this process in what is described by the “rocker-switch” alternative accessing model (Law, Maloney et al. 2008). Taking antiporter as an example, the transporter alternates between the inner facing conformation (Ci) and the outer facing conformation (Co). The Ci conformation has lower energy than the Co conformation (Huang, Lemieux et al. 2003, Law, Maloney et al. 2008) . In the first step of transport, the Co binds to a substrate in the outer environment. Because the energy of the Co conformation is higher than that of the Ci conformation, the substrate induced transporter conformation changes can move the substrate against

its gradient and the structure of the transporter changes to the Ci conformation. Later, the Ci binds to an ion in the cytoplasm and moves it to the outer environment. Because the transport of the ion is down its gradient, the transporter uses the ion's electrochemical potential energy to return to the high energy Co conformation (Law, Maloney et al. 2008).

ATP-binding Cassette (ABC) Superfamily

ABC type transporters are as important and widespread as MFS transporters. In *E. coli,* 5% of coding genes belong to the ABC transport systems (Rees, Johnson et al. 2009). This type of transporter is primary active transporter which transports the substrates against the concentration gradients and is energized by ATP hydrolysis (Davidson, Dassa et al. 2008). The ABC transport systems are not only important for the uptake of a variety of nutrients but they are also critical for the export of harmful solutes, e.g. toxins and drugs (Rees, Johnson et al. 2009).

ABC type transporters typically contain two transmembrane domains (TMD) with 6 α-helices in each domain and two intracellular nucleotide-binding domains (NBD) which are ATP binding components (Davidson, Dassa et al. 2008). Importers have an extra periplasmic-binding domain. The alternating binding and release of ATP with the NBD drives the conformational changes of TMD to move the substrate across the membrane.

High resolution protein tertiary structures are available for several ABC type

transporters (Locher, Lee et al. 2002, Hollenstein, Frei et al. 2007, Ward, Reyes et al. 2007). These protein structures correspond to different stages in the transport cycle, which gives us insights into the mechanism of ABC type transporters. The mechanism can be described by the alternating access model: The ABC transporters move substrates by changing conformations between the inward facing and outward facing states. This process is driven by hydrolysis of ATP. When the NBD domains are not bound to the ATP, the two NBD domains are more separate. In contrast, the ATP-bound NBD domains form stable closed dimers (Davidson and Chen 2004). The binding of substrates to the TMD domains, either directly or indirectly, induces the conformational changes of the NBD domains. The conformation changes facilitate binding of ATP and the formation of closed NBD dimers (Davidson and Chen 2004, Davidson, Dassa et al. 2008, Rees, Johnson et al. 2009). Then, the nucleotide-dependent conformation changes of the NBD domains induce the conformation changes of the TMD domains (Rees, Johnson et al. 2009). Later the ATP-free state is restored by hydrolyzing ATP and releasing phosphates (Davidson, Dassa et al. 2008).

PstSCAB and PhnCDET

Most soils contain only low concentrations of available phosphorous (primarily phosphate 0.1-10 μM) (Bieleski 1973) and *S. meliloti* has different types of phosphate transporters whose transcription is activated during growth under low phosphate

concentrations. These phosphate transport systems include PstSCAB and PhnCDET. PstSCAB is a phosphate specific transporter. PhnCDET is phosphonate transporter which is also capable of transporting phosphate and phosphites (Wanner and Metcalf 1992). PhnCDET also provides phosphorous for nodulation (Bardin, Dan et al. 1996).

There are some similarities between the two systems. 1) Both of them are high affinity Pi transporters. The Km values for Pi uptake via the *S. meliloti* PstSCAB system and PhnCDET are both 0.2 μM (Voegele, Bardin et al. 1997, Yuan, Zaheer et al. 2006). They are activated during growth at low phosphate concentrations while repressed when grown at high phosphate concentrations. 2) They both belong to ABC type transporters. There are multiple components involved in each transport system and each gene in the operon encodes a component, e.g. membrane component, ATP-binding component, and periplasmic-binding component. 3) Both of them are members of Pho regulon which consists of a number of phosphate assimilation related genes. The previously mentioned Ugp operon is another member of this operon.

The expression of most genes of the Pho regulon, including PstSCAB and PhnCDET, is controlled by the two component system PhoB/PhoR in Gram-negative bacteria (Yuan, Zaheer et al. 2006). PhoR is the Pi sensory histidine kinase which regulates PhoB's transcriptional factor activity as a DNA-binding response regulator (Hsieh and Wanner 2010). PhoR is autophosphorylated during Pi limitation and the autophosphorylated PhoR will phosphorylate PhoB at its N-terminal receiver domain,

then the C-terminal DNA binding domain of PhoB-P binds to the conserved Pho box motif in the promoters to initiate the transcription of target genes. Therefore, PhoB is essential to the expression of PstSCAB and PhnCDET systems and a *PhoB*$^{-}$ mutant will abolish the function of the two transport systems (Hsieh and Wanner 2010).

The PstSCAB system also requires PhoU for regulation of its expression. PhoU is the Chaperon-like PhoU/PhoB inhibitory protein downstream of *pstSCAB* in *S. meliloti* chromosome. The chromosomal location of PstSCAB-PhoU and PhoB/PhoR is illustrated in Figure 1. *pstS, pstC, pstA, pstB, phoU* and *phoB* are transcribed into a single transcript. PhoU is a member of PhoU family (Pfam ID: PF01895). PhoU and PhoU_div (Pfam ID: PF01865) families are the two members of the PhoU-like superfamily. The role of PhoU was predicted as a chaperon-like role because of the structural similarity between PhoU-like proteins from *Aquifex aeolicus* and *Thermotoga maritima* and the eukaryotic chaperone Hsp70 family (Liu, Lou et al. 2005, Oganesyan, Oganesyan et al. 2005). PhoU is hypothesized to act as an accessory protein which helps PhoR to activate the auto-dephosphorylation of PhoB-P to deactivate PhoB(Lamarche, Wanner et al. 2008).

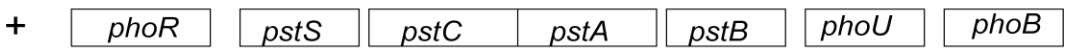

Figure 1. The chromosomal locations of *S. meliloti* pstSCAB-phoUandPhoB/PhoR.

Pap-Pit

The Pit system (Pi transport) is a low affinity Pi transporter found in many species of prokaryotes and eukaryotes. The Pit system has a lower affinity for Pi than

PstSCAB and PhnCDET transporters. The Km values for Pi uptake via *E. coli* PitA and PitB and *S. meliloti* Pap-Pit are about 2 μM (Voegele, Bardin et al. 1997, Harris, Webb et al. 2001) compared to ~0.2-0.4 μM for *E. coli* PstSCAB (Rosenberg, Gerdes et al. 1977) and 0.2 μM for *S. meliloti* PstSCAB (Yuan, Zaheer et al. 2006). Pit is a member of the Major Facilitator Superfamily and therefore functions as a single trans-membrane protein with 10 to 12 transmembrane helices. As a secondary transporter, Pit symports phosphate with another ion across the membrane. For example, *E. coli* PitA and PitB symport phosphate in the form of neutral phosphate metal complex with a H^+; Neurospora crassa Pit symports phosphate with Na^+. The Pit system may also serve to transport other substrates such as arsenate and tellurite (Elias, Abarca et al. 2012) in addition to phosphate.

In *S. meliloti*, *pit* (Smc02861) encodes for a 334 amino acid protein transcriptionally associated with an upstream gene originally designated as "*orfA"* and now "*pap*" (pit associated protein, Smc02862). *S. meliloti pap-pit* was first identified in a PhnCDET mutant which is unable to form nodules that fix nitrogen (Fix^-). One class of *phnCEDT* Fix^- suppressor mutations was identified by deleting a thymidine from a hepta-thymidine sequence 54bp upstream of *pap* transcription start site. Deletion of thymidine increased *pap-pit* transcription which restored nitrogen fixation in the PhnCDET mutants (Bardin, Voegele et al. 1998).

The *S. meliloti pap-pit* operon is repressed by Pi starvation and induced when phosphate is in excess (Pi 2 mM) (Bardin, Voegele et al. 1998). It is negatively regulated by PhoB which binds to Pho box in the promoter. When wild type *S.*

meliloti was grown in media containing excess Pi, *pap-pit* expression was higher than that in low Pi media, while a *phoB* mutant showed high constitutive *pap-pit* expression and the transcription level did not change in response to different Pi concentration in the media(Bardin, Voegele et al. 1998, Yuan, Zaheer et al. 2006). Unlike the *S. meliloti* Pap-Pit system, the *E. coli pitA* and *pitB* genes are believed to be constitutively expressed and independent of PhoB regulation (Rosenberg, Gerdes et al. 1977). Accordingly, no Pho box for PhoB binding was found in the promoter regions (Yuan, Zaheer et al. 2006).

S. meliloti pap gene lies upstream of *pit* and the adenosine of the *pap* stop codon, TGA, is shared with the *pit* start codon, ATG (Figure 2)(Bardin, Voegele et al. 1998). The pap gene appears to be co-transcribed with *pit*. *pap* encodes a 214-amino-acid protein and is a member of the Pfam PhoU_div family (Pfam ID: PF01865)(Punta, Coggill et al. 2012). Within the PhoU_div family, putative PhoU-like phosphate regulatory proteins from *Shewanella oneidensis* MR-1 (2IIU) and from *Bacteroides thetaiotaomicron* VPI-5482(3L39) have been crystallized and can be used as a model for *S. meliloti* Pap structure. The structures indicate that Pap protein is a six-helix bundle (Figure 3).

PhoU_div family and PhoU family are the only two members of the PhoU-like superfamily. They are distantly related to each other. *S. meliloti* Pap and PhoU also share some structural similarities. *S. meliloti* PhoU consists of two PhoU domains and each PhoU domain contains a three-helix bundle, so this protein also has six helices (Punta, Coggill et al. 2012). Therefore, the function and mechanism of PhoU could be

relevant for inferring Pap function as they presumably share some overlapping regulation mechanisms.

Shewanella oneidensis and *Streptomyces coelicolor* were also included in the study of *pap-pit*. *S. oneidensis* is a gram negative gamma-proteobacterium while *S. coelicolor* is a gram positive actinobacteium. *S. oneidensis pap-pit* (SO_3770 and SO_3771) and *S. coelicolor pap-pitH1* (SCO4137 and SCO4138) are analogous to *S. meliloti pap-pit*. Protein mass of Pap and Pit/PitH1 are also comparable among the three species of bacteria (*S. oneidensis* Pap is 226aa and Pit is 424aa; *S. coelicolor* Pap is 206aa and PitH1 is 332aa). Unlike *S. meliloti,* there are no overlapping nucleotides between *pap* and *pit* in the two species.

Zaheer showed that when *phoB::TnV* is transduced into *pap*$^{-}$ mutants to abolish PstSCAB and PhnCDET, no transductants could be recovered on the selective media, in spite of the intact *pit*, and this could be complemented if Pap is provided *in trans* by a plasmid (Zaheer and Finan, unpublished work). This indicates that only when *PhoB::TnV* is transduced into the strain carrying wild type *pap* and *pit* together can transductants be recovered. This indicates that Pap appears to be required for Pi uptake in *S. meliloti* (Zaheer and Finan, unpublished work).

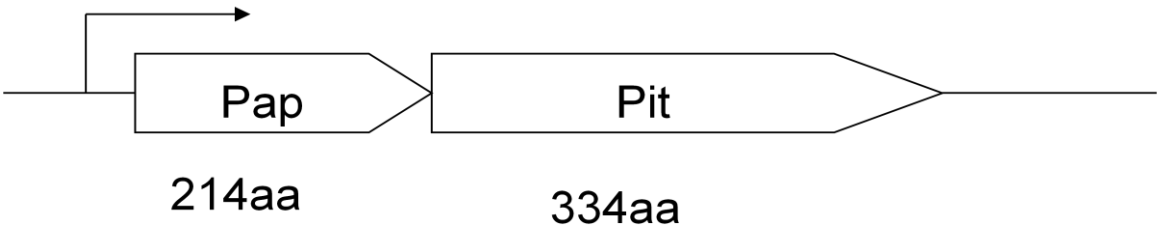

Figure 2. *S. meliloti pap-pit* operon and peptide sizes.

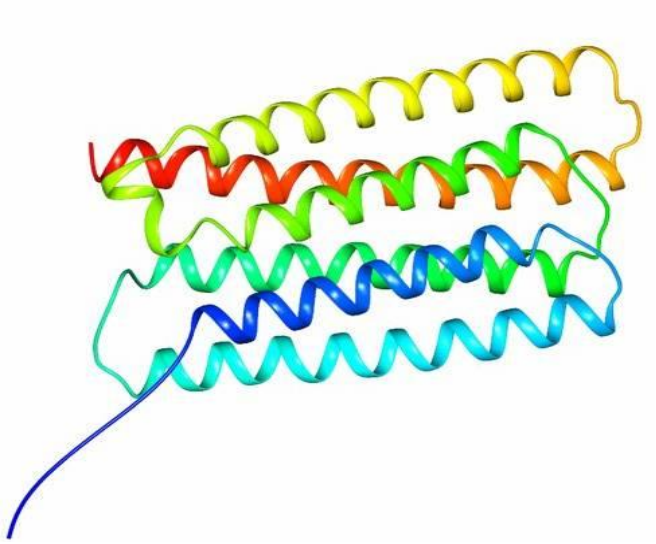

Figure 3. Inferred Pap 3D structure constructed with Swiss model. The template is Putative PhoU-like phosphate regulatory protein from *Bacteroides thetaiotaomicron* (PDB entry: 3I39). Six alpha-helices are indicated separately in different colors.

E. coli Pi Uptake Mutants

E. coli has four different types of Pi uptake systems including PstSCAB, PhnCDE, PitA and PitB. Three *E. coli* strains, MG1655, MT2006 and MT2016 were used in the study of *S. meliloti pap-pit* (Table 1). MG1655 is the wild type. MT2006 is a MG1655 derivative with all four types of Pi transporters deleted or replaced by antibiotics resistance cassettes that were Flp-recombinase excised for several of the mutant alleles. MT2016 is the same as MT2006 except the three additional phosphate-related genes, *phoA, yjbB* and *glpT*, were deleted (Motomura, Hirota et al. 2011).

Due to the lack of Pi transport systems, the two mutants fail to grow on media containing Pi as the sole source of phosphorus (Motomura, Hirota et al. 2011). However, they can transport phosphate when it is present in organic molecules such as glycerol-3-phosphate (G3P) via Ugp and GlpT or hexose-6-phosphate via UhpT

(Hayashi et al., 1964; Schweizer et al., 1982). Thus MT2006 and MT2016 can grow when 1mM G3P is present in the media. In this study, the Pi uptake mutants were used in complementation experiments to exclude the interference of all other types of Pi transporters in *E. coli*.

SNAP

It is assumed that *S. meliloti* Pit is localized in the cell membrane as a single trans-membrane transporter. However, Pap's exact function, location and its interaction with Pit are still unknown. It will be helpful to determine the localization of Pap in the cell in order to infer whether Pap and Pit interact physically. Unpublished results suggested that Pap is required and plays aregulatory role for the function of Pit in Pi uptake. It is also hypothesized to be localized in the cytoplasm along the cell membrane.

In this study, a visualization tag, SNAP tag, was used to locate Pap in the cell by fusing SNAP to the N terminus of Pap to construct a SNAP-Pap fusion protein. The SNAP tag used here is a ~20KD modified AGT (O^6-alkylguanine-DNA alkyltransferase), a human DNA repair protein. This protein binds rapidly and specifically with synthetic fluorophores linked to benzylguanine and a highly stable covalent bond is formed (Figure 4). The fluorescent signals can be detected via fluorescence microscope (Keppler, Pick et al. 2004).

As mentioned above, SNAP tag is a modified AGT. Therefore it can only be used in

the cells lacking O^6-alkylguanine-DNA alkyltransferase. AGT is not present in unicellular organisms. Since *S. meliloti* is unicellular organism, SNAP can be used in this study.

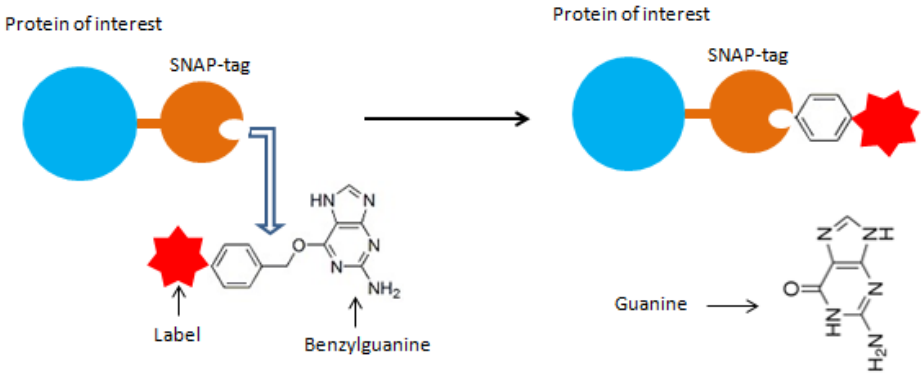

Figure 4. SNAP-tag fused to a protein of interest and forms a covalent bond with the label which is the substrate of benzylguanine.

Flp-FRT Recombination

Flp-FRT recombination strategy was used to make the *pap-pit* deletion strain in this study. FRT (Flp recognition target) is a short sequence recognized by Flp recombinase. The goal was to replace, by homologous recombination catalyzed by red recombinase, the *pap-pit* gene in a suicide plasmid with an antibiotic resistance cassette flanked by FRT sites. The resulting plasmid is mated into the *S. meliloti* wild type strain where it recombines via homologous recombination into the host genome. In this case, two regions of homology are present in the suicide plasmid;

one upstream of *pap-pit* and one downstream of *pap-pit*. Therefore, single or double crossover recombination may happen. If double crossover happens, the antibiotic resistance gene will replace the *pap-pit* genes in the chromosome and the Gm^r marker of the suicide plasmid will be lost. Then the resistance gene can be removed by Flp recombinase which catalyses the excision of the region between the FRT sites flanking it.

In this study, pKD13 was the template plasmid of resistance cassette flanked by FRT sites. The position of Kanamycin (Km^r) cassette, FRT sites and priming sites are indicated in the sequence can be found in Figure 16 in the *Appendix*. The scar that remains following excision of the Km^r cassette contains no translation signals for downstream genes and therefore is mainly used for the deletion of the entire operon or a single gene (Datsenko and Wanner 2000). The lambda red recombinase was from pKD46 and the expression is under the control of arabinose inducible promoter. pKD46 is a low copy number plasmid and can be cured easily (Datsenko and Wanner 2000). The suicide plasmid is pUCP30T whose double crossover recombination can be easily distinguished from single crossover as single crossover will produce Gm^r colonies while double crossover will produce Gm^s colonies.

This Work

Previous unpublished research suggested that Pap is required for the functionality of the Pap-Pit transport system in *S. meliloti* (Zaheer et al. unpublished work). However the exact function of Pap remains unknown. To help understand

what Pap does in the Pap-Pit system during Pi uptake, a series of complementation experiments were conducted based on the ability of the plasmids carrying *pap-pit* or *pit* from three species to complement the two *E. coli* Pi uptake mutants. To study the functional residues in Pap, 11 putative conserved amino acids were identified as functionally important sites for Pap function using bioinformatics approaches. These amino acids can be used for future mutagenesis experiment. The cellular location of Pap is also of great interest, so a SNAP tag was fused to Pap to help locate Pap with microscopic technology. A *S. meliloti pap-pit* deletion strain was also prepared.

MATERIAL AND METHODS

Growth Conditions

S. meliloti was grown in LBmc liquid media or LB agar (Bertani 1952). LBmc is LB containing 2.5 mM $MgSO_4$ and 2.5 mM $CaCl_2$. Antibiotics concentrations for *S. meliloti* grown on solid media were: streptomycin (Sm) 200 µg/ml, neomycin (Nm) 200 µg/ml, gentamycin (Gm) 60µg/ml. *E. coli* was grown in LB liquid media or LB agar. Antibiotic concentrations for *E. coli* grown in solid media were: ampicillin (Amp) 100 µg/ml, spectinomycin (Sp) 100 µg/ml, tetracycline (Tc) 5 µg/ml, kanamycin (Km) 20 µg/ml, gentamycin (Gm) 10 µg/ml, chloramphenicol (Cm) 10 µg/ml. 5-Bromo-4-chloro-3-indolyl β-D-galactopyranoside (X-gal) concentration used for blue white screen was 40 µg/ml. When necessary, 1 mM of glycerol-3-phosphate (G3P) was added to the media to restore growth. The antibiotics concentrations in liquid media for both strains were half of their concentrations in solid media.

The basic M9 minimal media contained 48 mM disodium phosphate, 22 mM monopotassium phosphate, 8.6 mM sodium chloride, 18.6 mM ammonium chloride, 20 mM mannitol as the carbon source, 1 mM $MgSO_4$, 0.25 mM $CaCl_2$, 0.005 µg/ml biotin and 10 ng/ml $CoCl_2$. The total phosphate concentration was 70mM and therefore it is a type of high Pi media. M9/IPTG media was M9 containing 0.5 mM IPTG. M9/G3P was M9 containing 1 mM G3P. M9/IPTG/G3P was M9 containing both 0.5 mM IPTG and 1 mM G3P. The stock solutions of biotin (0.2 mg/ml), $CoCl_2$ (0.1 mg/ml), G3P (200 mM), IPTG (100 mM) and mannitol (0.5 M) were sterilized by

filtration. Other ingredients were sterilized by autoclaving at 121°C for 20 minutes.

SOB and SOC media were prepared as described by Hanahan (Hanahan 1983). SOB and SOC both contain 2% Bactotryptone, 0.5% yeast extract, 10 mM NaCl, 2.5 mM KCl, 20 mM Mg salts (half $MgSO_4$ and half $MgCl_2$). In addition, SOC contains 20mM of glucose (Hanahan 1983).

Cloning

The target gene was PCR amplified with the corresponding forward and reverse primers which carried the same restriction sites as on the vectors. The PCR product was run on a 0.8% agarose gel and the DNA was recovered from the gel with a QIAquick gel extraction kit (QIAgen).

The recovered PCR product and vectors were separately double digested with the appropriate restriction enzymes (New England Biolab) overnight at 37°C. Then the double digested PCR product was purified with a QIAquick gel extraction kit (QIAgen) and eluted with 30 µL of EB Buffer provided by the kit to concentrate the DNA.

The purified restricted PCR product (insert) and vector were ligated by mixing 5µl of insert and 3µl of vector with 1µl T4 DNA ligase (New England Biolab) and 1µl 10 x T4 DNA ligase buffer (New England Biolab). The ligation mixture was then incubated at 16°C overnight. The next day, the ligation mixture was transformed into *E. coli* DH5α and plated on selective media containing appropriate antibiotics. If blue white

screening were applicable, the selective media were also supplemented with X-gal to screen for white colonies.

Plasmids were extracted from colonies by alkaline lysis as described in Molecular Cloning (Sambrook 2001) or by QIAprep spin Miniprep kits (QIAgen). The plasmids were digested with the same restriction enzymes and run on 0.8% agarose gel. If the insert could be seen on the gel at the correct size, the plasmid would be sent to the Mobix facility for sequencing .

Subcloning

The original plasmid pTH348 (Bardin, Voegele et al. 1998) was double digested with *EcoRV* (blunt end) and *HindIII* to get the 2.07 kb fragment which carries *S. meliloti pap-pit* with ~220 bp upstream of *pap* and ~150 bp downstream of *pit* (*Appendix* Figure 20).

pUC118 was double digested with *SmaI* (yield blunt end) and *HindIII*. Double digested pTH348 and pUC118 were mixed and concentrated into 30 µl by ethanol precipitation. 8 µl of the mixed DNA was ligated by adding 1 µl T4 DNA ligase (New England Biolab) and 1 µl 10 x T4 ligase buffer (New England Biolab). The ligation mixture was incubated at 16°C overnight and transformed into DH5α, and plated on appropriate selective media with X-gal. Plasmids from 8 white colonies were verified by digesting with *XmaI.* The presence of the 1.8 kb *XmaI-XmaI* fragment indicated a positive subclone and this plasmid was designated pTH2825 (Appendix Figure 21).

Complementation Experiments

Complementation of *E. coli* strains for Pi uptake.

Different plasmids as listed in the *Result* section were transformed into MG1655, MT2006 and MT2016 made competent by $CaCl_2$ treatment as described in Molecular Cloning (Sambrook 2001). Transformants were selected by plating on LB media containing 1 mM glycerol-3-phosphate and the appropriate antibiotics. Transformants were streak-purified twice on LB media containing 1 mM G3P and the antibiotic and streaked onto M9 minimal media to check for complementation. Growth was determined after 3 days of incubation at 30°C.

In this study, four types of M9 media, M9, M9/IPTG, M9/G3P and M9/IPTG/G3P were used in the complementation experiment. 20 mM mannitol, instead of the commonly used glucose, was used as the carbon source to prevent catabolite repression of the plasmid p*lac* promoter. As described in *growth conditions*, M9/G3P and M9/IPTG/G3P contain 1 mM of G3P. Therefore all the three *E. coli* strains can grow on them. By contrast, M9 and M9/IPTG only contain inorganic phosphate, so only MG1655 can grow on them, but MT2006 and MT2016 cannot. However if MT2006 and MT2016 contained plasmids that complemented the mutants defective in Pi uptake, they would be able to grow on these media as well. Based on this, the criterion for judging complementation was: if MT2006 and MT2016 containing a particular plasmid could grow on M9 or M9/IPTG, this clone was considered as complementing the mutants. If the MT2006 and MT2016 containing the plasmid only

grew on M9 containing G3P, this plasmid was not considered to complement.

Complementation of *S. meliloti* for Pi Uptake

To check if a plasmid complemented *S. meliloti Δpap* (RmP1628), *Δpit* (RmP1629) or *Δpap-pit* (RmP3151) strains for Pi uptake, the plasmid was first conjugated into *S. meliloti*. The transconjugants were selected on LB with the appropriate antibiotics. *phoB::TnV* (neomycin resistant) from a RmP560 ϕM12 lysate was transduced into the transconjugants to eliminate the Pi uptake via the PstSCAB and PhnCDET Pi-transporters and plated on LB with 200 µg/ml neomycin. If transductants were recovered on the plate, this plasmid was considered capable of complementing for Pi uptake as the Pi uptake by Pap-Pit is restored.

Growth Curves

1 ml of overnight LB culture with antibiotics was washed twice with 0.85% NaCl and resuspended in 1 ml 0.85% NaCl. The OD_{600} was measured and a certain volume of the cell suspension was transferred to 5 ml of M9, M9/IPTG and M9/G3P, respectively, making the initial OD_{600} at 0.05 for each sample. OD_{600} was read every four hours for 20 consecutive hours at 30°C with agitation.

Identification of Functionally Important Amino Acids in Pap using Bioinformatic Approaches

Over one million protein sequences from alpha-proteobacteria were downloaded from UniProt (Jain, Bairoch et al. 2009). HMMer (Finn, Clements et al. 2011) was used to annotate the protein sequences. After annotation, 57 protein sequences carrying PhoU_div as the most significant domain were collected. The 57 sequences were aligned with MUSCLE (Edgar 2004). The multiple sequence alignment file generated by MUSCLE was then applied to ConSurf (Armon, Graur et al. 2001) to calculate the conservation scores of amino acids in the Pap protein. Because more insights on functionally important amino acids can be sometimes obtained using information from protein tertiary structure, SWISS-MODEL (Schwede, Kopp et al. 2003) was used to predict the protein tertiary structure of the *Sinorhizobium meliloti* PhoU_div protein using *Bacteroides thetaiotaomicron* VPI-5482, a putative PhoU-like phosphate regulatory protein (PDB entry: 3L39), as a template. Then, the conservation score was mapped to its corresponding amino acid in the predicted tertiary structure. In the output of ConSurf, different degrees of conservation were indicated by numbers ranging from 1 to 9 and each number has a corresponding color in which 9 was the highest conservation score and was represented by purple. ConSurf also provided a confidence interval to measure the reliability of the estimated conservation score. Since we were only interested in the most conserved amino acids with the highest confidence level, sites with confidence interval (9, 9) were considered to be most conserved. In addition, exposed amino acids were

identified using ASAview (Ahmad, Gromiha et al. 2004) with the cutoff of relative solvent accessibility set at 0.2 (20% of the amino acid surface is exposed). Exposed surface amino acids are more likely to be involved in important functions while buried ones are not. Therefore, exposed amino acids whose confidence interval of conservation score was (9, 9) were considered to be functionally important.

SDS Polyacrylamide Gel Electrophoresis and Membrane Transfer

In this study, the concentration of Bis-acrylamide used for protein gels is 12%. The stacking gel and separating gel were prepared as described in Molecular Cloning (Sambrook 2001) . 1 ml of overnight cell culture was spun down and resuspended in SDS loading dye, then boiled for 5 minutes to lyse the cells. The lysed cells were centrifuged for 5 minutes at 13,000 rpm. 8 µl of the supernatant from each sample was loaded and run at 150 V until the loading dye reached the bottom of the gel.

The protein in the gel was then transferred to PVDF membrane using a Bio-Rad semi-dry transfer cell at 10 V for 60 min. The preparation of the “sandwich” with two pieces of extra-thick blocking paper, gel and membrane was set up asspecified in the Bio-Rad Trans-Blot SD Cell Manual.

Western Blotting

After the protein was transferred to the membrane, the PVDF membrane was

blocked in 5% skim milk in TBST buffer (100 mM Tris-Cl pH 7.5; 150 mM NaCl; 0.05% Tween) for 1-2 hrs at room temperature or overnight at 4°C. The membrane was then incubated with 30 ml of TBST containing 1.5% skim milk and 6 µl of primary anti-Pap antibody made in rabbit for 1-2 hrs with shaking at room temperature. Afterwards, the membrane was washed three times, 10 minutes for each wash, using TBST buffer before incubating with 30 ml TBST containing 1% skim milk and 10µl of Bio-Rad goat-anti-rabbit IgG secondary antibody (1: 3000). Again the membrane was washed three times (10 minutes for each wash) with TBST buffer.

After the three washes, the membrane was equilibrated for 5 min in alkaline phosphatase (AP) buffer (0.1 M Tris-Cl, pH 9.5; 0.1 M NaCl; 5 mM MgCl2) and then developed in 15ml AP color developing buffer (99 µl of 50 mg/ml nitro blue tetrazolium chloride (NBT) stock solution and 50 µl of 50 mg/ml 5-Bromo-4-chloro-3-indolyl phosphate (BCIP) stock solution in 15ml AP buffer) in the dark until the development of a dark purple color.

Transformation

1-2 µl of plasmid DNA was added to 200 µl aliquots of DH5α competent cells in 1.5 ml Eppendorf tubes and incubated on ice for 20 minutes. The cells were then heat shocked at 42°C for 1.5 min and replaced on ice for 1 min. 1 ml of LB was added to the tube and the culture was incubated with agitation for 1 hour. After incubation, 150 µl was plated onto appropriate selective media.

Conjugation

To transfer a plasmid into *S. meliloti* recipients, 1 ml of the *E. coli* donor, the helper strain MT616 carrying the mobilizing plasmid pKD600. The overnight culture of the recipient *S. meliloti* was washed three times with 0.85% NaCl, respectively. 25 µl of each washed culture was mixed and spotted onto an LB plate to make the tri-parental mating spot. The mating spots were incubated at 30°C overnight and plated on LB with appropriate antibiotics to select for *S. meliloti* recipient carrying the plasmid.

Transduction

Phage lysates were made by adding 100 µl of ϕM12 phage lysate to log phase *S. meliloti* cultures, and incubating the culture-phage mixture overnight at 30°C. 100 µl chloroform was added to the phage lysate to kill the surviving bacteria. The phage lysate was diluted 20 times with LB and stored at 4°C. For transduction, 300 µl of diluted phage lysate and *S. meliloti* recipient overnight cultures were mixed and incubated at 30°C for 20 minutes. 100 µl of the mixture was plated on LB with appropriate antibiotics. The recipient culture and phage lysate were also plated individually as negative controls.

Construction of SNAP-Pap Fusion Protein

S. meliloti pap-pit was PCR amplified from wild type strain RmP110 and cloned

into pENTR4 SNAPf (gift from Dr. Kieran Finan, Appendix Figure 22) between *KpnI* and *XbaI* with *pap* start codon ATG removed. The insert fragment is in frame with the upstream SNAP sequence as shown in Figure 5. The resulting plasmid was labelled as pTH2867. SNAP-*pap-pit* was then PCR amplified from pTH2867 and inserted into pUCP30T between *XbaI* and *HindIII*. The resulting plasmid was annotated as pTH2868.

The 200bp upstream region of *pap* (nt: 216762-216563) including *pap* promoter was PCR amplified and cloned into pTH2868 upstream of *SNAP-pap-pit* between *SacI* and *XbaI* to make pTH2869.

The plasmids were confirmed by DNA agarose gel electrophoresis after double digestion, sequencing and the SNAP-Pap expression from pTH2868 was confirmed by western blot. pTH2869 was conjugated into RmP1628 (RmP110 *Δpap*) and RmP1629 (RmP110 *Δpit*) via the helper strain MT616 to make the two *S. meliloti* strains RmP3149 and RmP3150 which express SNAP-Pap fusion protein. The strains were verified by colony PCR using different sets of primers (Figure 9, Figure 10) and by western blotting (Figure 11).

ATGGACAAAGACTGCGAAATGAAGCGCACCACCCTGGATAGCCCTCTGGGCAAGCTGGAACTGTC
TGGGTGCGAACAGGGCCTGCACCGTATCATCTTCCTGGGCAAAGGAACATCTGCCGCCGACGCCG
TGGAAGTGCCTGCCCCAGCCGCCGTGCTGGGCGGACCAGAGCCACTGATGCAGGCCACCGCCTGG
CTCAACGCCTACTTTCACCAGCCTGAGGCCATCGAGGAGTTCCCTGTGCCAGCCCTGCACCACCC
AGTGTTCCAGCAGGAGAGCTTTACCCGCCAGGTGCTGTGGAAACTGCTGAAAGTGGTGAAGTTCG
GAGAGGTCATCAGCTACAGCCACCTGGCCGCCCTGGCCGGCAATCCCGCCGCCACCGCCGCCGTG
AAAACCGCCCTGAGCGGAAATCCCGTGCCCATTCTGATCCCCTGCCACCGGGTGGTGCAGGGCGA
CCTGGACGTGGGGGGCTACGAGGGCGGGCTCGCCGTGAAAGAGTGGCTGCTGGCCCACGAGGGCC
ACAGACTGGGCAAGCCTGGGCTGGGT cct gca ggc gga tcc ggt acc CTC GGC CTG TTT CGC AAG CTC CTC CCC ...

Figure 5. The sequence showing *pap* downstream of SNAP in frame. SNAP open reading frame was shown in bold uppercase letters. The sequence in lowercase encodes for seven amino acids connecting SNAP and Pap. The underlined region is *KpnI* site which was used to clone *pap-pit* downstream of SNAP. The shaded region in uppercase is *Pap* coding sequence starting from the fourth nucleotide as Pap start codon ATG was removed so as to ensure a successful fusion with SNAP.

Deletion of *pap-pit* in *S. meliloti*

Induction of λ-red recombinase and making electrocompetent cells

pTH2824 (*S. meliloti pap-pit* with 500bp upstream and downstream region in pUCP30T) was prepared as described in the *cloning* section. It was transformed into M1420 which carries pKD46 (ampicilin resistant) that expresses λ-red recombinase under L-arabinose induction. The transformants were annotated as M2095. M2095 was grown up in 50 ml of SOB media with 50 µg/ml ampicilin, 5 µg/ml gentamycin and 20mM L-arabinose at 30°C until OD_{600} reached 0.6. The cells were then washed three times with ice-cold 10% glycerol and concentrated 100 fold. The electrocompetent cells were stored at -80°C.

Electroporation of the Kanamycin cassette into M2095

The Kanamycin cassette flanked by FRT sites was PCR amplified using pKD13 as template. The PCR product were eluted and purified from the 0.8% agarose gel with a QIAquick gel extraction kit (QIAgen) and treated with DpnI to digest the original template plasmid. After digestion the PCR product was again purified using the same kit.

50 µl of electrocompetent M2095 and 400 ng of the PCR product were mixed in the cuvette and shocked using Bio-Rad MicroPulser Electroporator at 2.5 kV. After electroporation, 1 ml of SOC media with 1 mM of L-arabinose was added to the shocked cells immediately followed by 30 °C incubation with agitation for two hours, then plated on LB media with 20 µg/ml of kanamycin and 10 µg/ml of gentamycin. A new plasmid pTH2897 will be made resulted from the double crossover between pTH2824 and the kanamycin cassette, and only the cells carrying pTH2897 would grow on the selective media. The colonies selected were streak-purified and incubated at 37 °C to eliminate pKD46 which is temperature sensitive. The resulting strain was annotated as M2096 (M1420 with pTH2897).

Recombination of the pTH2897 into RmP110 to eliminate *pap-pit*

pTH2897 was transferred into *S. meliloti* RmP110 by conjugation. The colonies in which *pap-pit* had been replaced by the kanamycin cassette were selected on LB containing 200 µg/mg neomycin. 100 colonies were then patched to LB with 60 µg/ml gentamycin and also to LB with 200 µg/mg neomycin at the same time to

screen for the double crossover which would be neomycin resistant and gentamycin sensitive.

Elimination of Kanamycin cassette

The Flp expression plasmid pTH1944 (Tetracycline resistant) was mated from M842 into M2096. Colonies that lost neomycin resistance due to excision between FRT sites, and elimination of the kanamycin cassette, were isolated. The elimination of kanamycin cassette was confirmed by colony PCR and sequencing. The resulting strain was annotated as RmP3151.

Polymerase Chain Reaction (PCR)

Primers for each PCR reaction were designed with GeneRun software and ordered from Mobix facility. The primers are resuspended and diluted to a final concentration of 10 µl in ddH_2O. The concentration of each component for PCR reaction is as follows, 1 x buffer, dNTP 200 µM, MgSO4 2mM, each primer 0.4 µM, genomic DNA template 100 ng/25µl and Taq polymerase 1 unit/25 µl.

The PCR cycle starts with 4 minutes of template denaturing at 94°C, followed by 30 cycles of 30 seconds at 94°C (melting) and 30 seconds at corresponding annealing temperature and a certain period of time at 72°C (extension) depending on the size of the fragment being amplified. After the last cycle a 7 minutes extension at 72°C was conducted.

For colony PCR, a single colony was resuspended in 100 µl of ddH_2O and 5µl was used as DNA template in each reaction.

Results

A list of the strains and plasmids involved in the complementation of *E. coli* Pi uptake mutants are shown in Table 1 with a brief description.

Table 1. Strains and plasmids for the complementation experiment.

Strains or Plasmids	Description	References or sources
***E. coli* strains**		
MG1655	Wild-type strain; F^- *arcA*-1655 *fnr*-1655	Rao et al, 1998
MT2006	MG1655*ΔpitB::frt ΔpitA::frt ΔphnC::frt Δ(pstSCAB-phoU)560::*Km^r	Motomura et al, 2011
MT2016	MG1655*ΔpitB::frtΔpitA::frt ΔphnC::frt Δ(pstSCAB-phoU)560*::Km^r *ΔphoA::frt Δ yjbB::frt Δ glpT::frt*	Motomura et al, 2011
***S. oneidensis* strains**		
MR-1	wildtype; Gamma-proteobacteria, metabolically versatile Gram negative bacterium	
Plasmids		
pMW119	Low copy cloning vector, Amp^r, pSC oriV,IPTG inducible *lac* promoter, a gift from Dr. Akio Kuroda	Kuroda, 2011
pRK7813	RK2 derivative carrying pUC9 polylinker and cos site; Tc^r	Jones, 1987
pUC118	Cloning vector; IPTG inducible *lac* promoter, Amp^r	Vieira et al, 1987
pTRsc	Broad host range expression plasmid; $Spec^r$; IPTG inducible *trc* promoter pBR322 and pVS1 oriV	Finan lab collection
pTH347	pRK7813 containing 2.6 kb *EcoRI* partial fragment (760bp upstream sequence of *pap* plus 1650bp *pap-pit* sequence plus 150bp downstream sequence of *pit)*	Bardin et al, 1998
pTH348	The same *EcoRI* fragment as pTH347 cloned into pRK7813 in the opposite orientation	Bardin et al, 1998

pTH2569	*S. meliloti orfA-pit* CDS cloned in pTRsc with *PacI* and *HindIII*	Zaheer et al.
pTH2571	*Streptomyces coelicolor pap-pitH1* cloned in pTRsc with *PacI* and *HindIII*	Zaheer et al.
pTH2631	*Streptomyces coelicolor pitH*1 CDS cloned in pTRsc with *PacI* and *HindIII*	Zaheer et al.
pTH2825	The 2.07kb fragment containing *S.meliloti pap-pit* from pTH348 and ligated into pUC118	This study
pTH2826	*S.meliloti pap-pit* cloned into pUC119 via *HindIII* and *XbaI*	This study
pTH2827	*S. meliloti pap-pit* cloned in pRK7813 via *HindIII* and *BamHI*	This study
pTH2828	*S.meliloti pap-pit* cloned into pMW119 via *HindIII* and *XbaI*	This study
pTH2829	*S. meliloti pit* cloned into pMW119 via *HindIII* and *XbaI*	This study
pTH2863	*S. oneidensis pap* cloned in pTRsc via *PacI* and *HindIII*	This study
pTH2864	*S. coelicolor pap* cloned into pUC119 via *HindIII* and *XbaI*	This study
pTH2871	*S. oneidensis pap-pit* cloned in pTRsc via *PacI* and *HindIII*	This study
pTH2872	*S. oneidensis pap-pit* cloned in pMW119 via *HindIII* and *XmaI*	This study
pTH2873	*S. oneidensis pit* cloned into pMW119 via *HindIII* and *XmaI*	This study

Complementation of clones for *E. coli* Pi uptake mutants

The clones in Table 1 were prepared using vectors of different copy number and *pap-pit, pap* or *pit* fragment from three species, and were tested for their ability to complement the *E. coli* uptake mutants as described in *Material and Methods*. Among the three vectors, pTRsc vector appeared to allow the mutants to grow to a low degree. Therefore, growth curves were performed to illustrate the complementation effect of whatever insert fragment cloned into pTRsc (*Appendix* Figure 18**,** Figure 19).

S. meliloti

The complementation results are listed in Table 2 with growth speed indicated by the number of "+". pTH2825 (pUC118 carrying *S. meliloti pap-pit* with ~220bp upstream and ~150bp downstream region) complemented the *E. coli* mutants on both M9 and M9/IPTG plates containing mannitol. pTH2569 (pTRsc carrying *S. meliloti* the *pap-pit* coding sequence) complemented the mutants only on M9/IPTG plates. pTH2827 and pTH2828, both of which are based on low copy number vectors pRK7813 and pMW119, and which carry *pap-pit,* did not complement. The insert fragment in pTH2828 was then cloned into the high copy pUC119 vector to make pTH2826. Unlike pTH2828, pTH2826 appeared to allow the host mutants to grow on both M9 and M9/IPTG.

It was hypothesized that pTH2827 and pTH2828 did not complement because the low copy number of the vectors in the host cells result in low levels of Pap-Pit expression. To confirm the hypothesis, a western blot analysis was performed using anti-Pap antibody. As shown in Figure 6, Pap was detected in MG1655 carrying pTH2825 and the induced MG1655 carrying pTH2569, but it could not be detected in the lysate of MG1655 containing pTH2827, pTH2828 and non-induced pTH2569. This coincides with the complementation results: MG1655 carrying pTH2825 which complemented the mutants showed obvious Pap expression. The plasmid pTH2569 that requires IPTG induction to complement only showed Pap in the IPTG induced culture lysate but not in the non-induced. In contrast, MG1655 carrying pTH2827 or pTH2828, neither of which complemented, did not show any detectable Pap protein

in western blots.

The mutants carrying pTH2568 (*S. meliloti pit* in pTRsc) formed mucoid colonies on M9/IPTG. Without IPTG, pTH2568 was unable to allow growth of the mutants on M9 medium. pTH2829 (*S. meliloti pit* cloned in pMW119) did not allow growth of the host mutants MT2006 and MT2016, possibly due to the absence of Pap and/or the low copy number of the vector. pTH2567 (*S. meliloti pap* in pTRsc) only complemented the mutants to a very low degree, similar to that of the empty pTRsc.

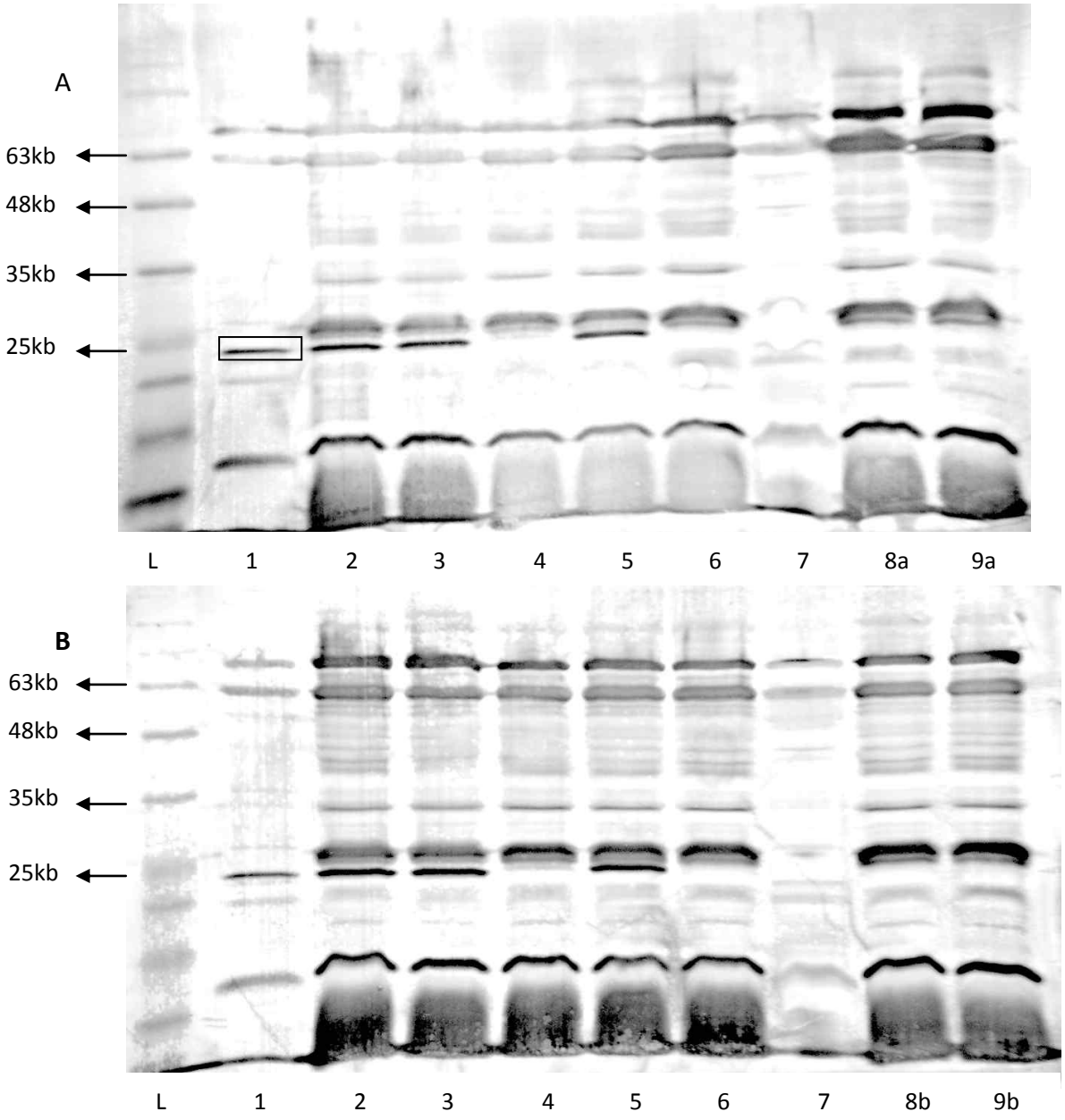

Figure 6. Western blot result of Pap expression from a number of clones involved in the *S. meliloti* complementation experiment. Blots were probed with anti-Pap antibody prepared from rabbit. It can be seen that Pap is not detectable from the two clones (lanes 8a, 9a, 8b, 9b) that did not complement. Wild type Pap is at ~23kd as indicated by the box. The cell lysate in each lane is: 1, *S.meliloti* RmP110; 2, *E. coli* MG1655 carrying pTH2825, non-induced culture; 3, MG1655 carrying pTH2825, induced; 4, MG1655 carrying pTH2569, non-induced culture; 5, MG1655 carrying pTH2569, induced culture; 6, MG1655; 7, *S. meliloti* RmP1628 (RmP110 Δpap); 8a, MG1655 carrying pTH2828, non-induced; 9a, MG1655 carrying pTH2828, induced. 8b, MG1655 carrying pTH2827, non-induced; 9b, MG1655 carrying pTH2827, induced.

S. oneidensis

pTH2872 (*S. oneidensis pap-pit* in pMW119) complemented the mutants on M9 and M9/IPTG plates. To confirm, pTH2871 (*S. oneidensis pap-pit* in pTRsc) was made and it was also found capable of complementing the mutants on M9. Surprisingly, when IPTG is present in the plates, pTH2871 appears to be lethal because the cells, including the wild type MG1655, which contain pTH2871 could not grow on the plate, no matter whether glycerol-3-phosphate is present. Therefore, the IPTG induction of pTH2871 appeared to be lethal to the *E. coli* host cells. pTH2873 (*S. oneidensis pit* in pMW119) complemented the mutants on M9/IPTG to an extremely low degree. *S. oneidensis pap* in pTRsc improved growth slightly, perhaps also due to the pTRsc vector.

S. coelicolor

pTH2571 (*S. coelicolor pap-pitH1* in pTRsc) complemented the mutants on both M9 and M9/IPTG. pTH2631 (*S. coelicolor pitH1* in pTRsc) allowed the mutants to

grow on M9, but became lethal to the host cells when induced by IPTG as it inhibited the growth of the three strains including the wild type MG1655 on IPTG containing media. pTH2864 (*S. coelicolor pap* in pUC119) did not show complementation effect. However, when pTH2864 and pTH2631 are both present in the *E. coli* mutants, the lethality of pTH2631 is eliminated, which was indicated by the restored wild type growth. Further, the two plasmids together allowed the mutants to grow on M9/IPTG.

Table 2. Complementation results of the plasmids for the *E. coli* Pi uptake mutants.

Plasmids	**Growth**	**Conditions**
empty vectors		
pTRsc(medium copy)	+/-	
pUC119(high copy)	-	
pMW119(low copy)	-	
S. meliloti		
pTH2825 (*S. meliloti pap-pit* in pUC118)	+++	
pTH2826 (*S. meliloti pap-pit* in pUC119)	++	
pTH2569 (*S. meliloti pap-pit* in pTRsc)	++	requires IPTG
pTH2827 (*S. meliloti pap-pit* in pRK7813)	-	
pTH2828 (*S. meliloti pap-pit* in pMW119)	-	
pTH2567 (*S. meliloti pap* in pTRsc)	+/-	
pTH2568 (*S. meliloti pit* in pTRsc)	mucoid	when IPTG is present
	+/-	on M9
pTH2870 (*S. meliloti pit* in pRK7813)	-	
pTH2829 (*S. meliloti pit* in pMW119)	-	
S. oneidensis		
pTH2871 (*S. oneidensis pap-pit* in pTRsc)	+++	on M9
	Lethal	when IPTG is present
pTH2872 (*S. oneidensis pap-pit* in pMW119)	+++	
pTH2863 (*S. oneidensis pap* in pTRsc)	+/-	
pTH2873 (*S. oneidensis pit* in pMW119)	+	requires IPTG
S. coelicolor		
pTH2571 (*S. coelicolor pap-pitH1* in pTRsc)	++	
pTH2864 (*S. coelicolor pap* in pUC119)	-	
pTH2631 (*S. coelicolor pitH1* in pTRsc)	++	on M9
	Lethal	when IPTG is present
pTH2864 and pTH2631	++	requires IPTG

The first column is the plasmids which had been transformed into MG1655, MT2006 and MT2016 for complementation experiments. The growth speed of the mutants is indicated by a certain number of "+" and was determined after three days of incubation at 30°C. +++ represents the wild type growth speed on M9 containing 20mM mannitol as the carbon source. +/- indicates very slow growth speed. – indicates no growth. The growth of MT2016 carrying some clones tended to be repressed by glycerol-3-phosphate (data not shown in the table).

Eleven amino acids in Pap were identified as being functionally important

S.meliloti Pap protein appears to be a compact globular protein containing six alpha-helices which are interconnected by loops (Figure 3). The six alpha-helices are nearly antiparallel to each other, forming an alpha-helix bundle. 18 amino acids including 11 exposed amino acids and 7 buried amino acids were identified as being conserved. After being mapped to the protein, the conserved amino acids (purple) clustered together in the tertiary structure to form three patches on one protein face (Figure 8) although they were not contiguous in the primary sequence (Figure 7). Furthermore, the E/DXXXD conserved motif occurred five times in the protein sequence. In the *S. meliloti* Pap protein sequence there were eleven exposed amino acids (E54, D58, T74, F75, R78, D90, D93, D160, E193, D197, D201) which were found to be conserved in other Pap proteins and thus were potentially important for Pap function. Those residues were targeted as candidates for site-directed mutagenesis of Pap.

Table 3. A list of conserved sites predicted by ConSurf.

Position	Amino acid	Score (normalized)	Color	Confidence interval colors	Residue variety	Relative solvent accessibility
54	**E(Glu)**	-1.245	9	9,9	E	0.228960
57	A(Ala)	-1.187	9	9,9	A,C	0.000000
58	**D(Asp)**	-1.254	9	9,9	D	0.380875
74	**T(Thr)**	-1.134	9	9,9	M,T,I	0.245106
75	**F(Pro)**	-1.099	9	9,9	R,P	0.514431
78	**R(Arg)**	-1.164	9	9,9	T,R	0.392940
81	I(Ile)	-1.115	9	9,9	A,I,V	0.000000
84	L(Leu)	-1.103	9	9,9	M,L	0.032766
89	D(Asp)	-1.254	9	9,9	D	0.076175
90	**D(Asp)**	-1.132	9	9,9	D,K	0.380875
93	**D(Asp)**	-1.165	9	9,9	D,G	0.283925
156	E(Glu)	-1.245	9	9,9	E	0.114480
160	**D(Asp)**	-1.254	9	9,9	D	0.339325
193	**E(Glu)**	-1.163	9	9,9	D,E	0.269028
197	**D(Asp)**	-1.185	9	9,9	D,N	0.477825
201	**D(Asp)**	-1.139	9	9,9	D,R	0.533225
202	V(Val)	-1.109	9	9,9	C,L,V	0.039036
203	A(Ala)	-1.115	9	9,9	A,G	0.027222

11 exposed amino acids with the highest conservation score (9) are highlighted in purple. 7 buried amino acids with the highest conservation score, 9, are highlighted in blue. Confidence interval (9, 9) indicates that the estimated conserved score (9) is highly reliable.

>sp|O30498|PITX_RHIME PhoU_div

1 MLGLFRKLLPREDRFFDLFADHSRTVMGAAEALNALLAGG

41 PDIESHCDRIVAL**E**NEA**D**EITREVLLAVRRSFI**TP**FD**R**GD

81 IKDLIQSMD**D**AI**D**MMHKTVKTIRLYEQKSFDPGMQAMGAA

121 VVEAAHLVAEAIPLLSRIGANAHRLSAIAEEVTHVEDRS**D**

161 QLHEQGLKDLFQRHGASNPMAYIIGSEIYGEL**E**KVV**D**RFE

201 **D**VANEISGIVIENV

Figure 7. *Sinorhizobium meliloti* Pap protein sequence showing the position of the conserved amino acids in the primary sequence. The 11 purple bold amino acids are the conserved surface amino acids in the sequence. The 7 underlined blue amino acids are conserved buried amino acids in the sequence.

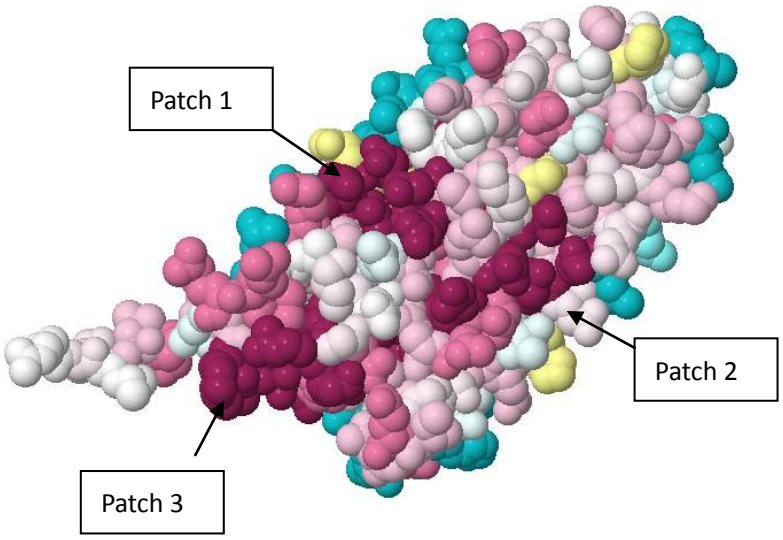

Figure 8. Spacefilling model of Pap generated by ConSurf. Amino acids of different conservation scores are shown with different colors. Purple represents the highest level of conservation. Three conserved patches (purple areas) are shown on the molecular surface. Distribution of the 11 surface conserved amino acids is: E(Glu)54, D(Asp)58, D(Asp)90, D(Asp)93 in Patch 1; D(Asp)160, E(Glu)193, D(Asp)197, D(Asp)201 in Patch 2; T(Thr)74, F(Pro)75, R(Arg)78 in Patch 3.

Validation of the plasmids carrying SNAP-*pap*

Plasmid pTH2868 carrying the SNAP-*pap* fusion and *pit* was found to complement the two *E. coli* mutants MT2006 and MT2016, indicated by the growth of MT2006 (pTH2868) and MT2016 (pTH2868) on M9 and M9/IPTG. Plasmid pTH2869 is almost the same as pTH2868 except that it also carries the 200 bp sequence which includes the *S. meliloti pap* promoter region. However it did not appear to complement the mutants.

Western blotting was performed to determine SNAP-Pap-Pit expression from the two plasmids prepared (Figure 11). Cells carrying pTH2868 show Pap shifting from 23KD to ~40KD presumably due to the presence of the SNAP fusion whereas those carrying pTH2869 did not show any bands at the expected size.

Validation of the two strains carrying SNAP-*pap* (RmP3149 & RmP3150)

Two *S. meliloti* strains RmP3149 and RmP3150 were constructed by recombining SNAP-*pap*-pit into RmP1628 (RmP110 *Δpap*) and RmP1629 (RmP110 *Δpit*), respectively, as described in *Material and Methods*, to express SNAP-Pap from chromosome. The expected genotypes of RmP3149 and RmP3150 were confirmed at first by colony PCR with primers targeting SNAP gene (Figure 9). In Figure 9, DNA fragments of expected size as specified in Figure 10 were successfully amplified from RmP3149 and RmP3150 with primers targeting SNAP gene, while RmP1628 and RmP1629 did not show PCR product. Further, western blot was performed to confirm that there is actual protein expression of the SNAP-Pap fusion (Figure 11). In RmP3149 cell lysate, a band at ~40KD (the same size as the SNAP-Pap expressed from pTH2868) was detected. RmP3150 shows a band at ~23KD (wild type Pap molecular weight) in addition to a band at ~40KD. Complementation experiment was also performed to show the ability of pTH2868 to complement RmP1628 and RmP1629 by transducing *phoB::TnV* into RmP3149 and RmP3150. The results showed that transductants could be recovered when *phoB::TnV* is transduced into RmP3150, but no transductants were observed on the plates when *PhoB::TnV* is transduced into RmP3149.

Table 4. Strains and plasmids involved in SNAP fusion construction.

Plasmids and Strains	Description	References or sources
Plasmids		
pENTR4 SNAPf	High copy number entry vector carrying SNAP tag sequence, pBR322 oriV, Km^R	K. Finan
pTH2867	pENTR4 SNAPf carrying pap-pit fragment between *KpnI* and *XbaI* and in frame with SNAP, *pap* start codon ATG removed	This study
pTH2868	SNAP-pap-pit PCR amplified from pTH2867 and cloned into pUCP30T between *XbaI* and *HindIII*, Gm^R	This study
pTH2869	200bp upstream of *pap* was PCR amplified and cloned into pTH2868 between *SacI* and *XbaI* upstream of SNAP-pap-pit	This study
***E. coli* strains**		
MG1655	Wild-type strain; F^- *arcA*-1655 *fnr*-1655	Rao et al, 1998
MT2006	MG1655*ΔpitB::frt ΔpitA::frt ΔphnC::frt Δ(pstSCAB-phoU)560::*Km^r	Motomura et al, 2011
MT2016	MG1655*ΔpitB::frtΔpitA::frt ΔphnC::frt Δ(pstSCAB-phoU)560*::Km^r *ΔphoA::frt Δ yjbB::frt Δ glpT::frt*	Motomura et al, 2011
***S. meliloti* strains**		
RmP110	Rm1021 with changed wild-type *pstC*	Yuan 2006
RmP560	RcR2011 *phoB::TnV*	Lab stock
RmP1628	RmP110 *Δpap*	Zaheer et al. unpublished work
RmP1629	RmP110 *Δpit*	Zaheer et al. unpublished work
RmP3149	RmP1628 with pTH2869 recombined into the chromosome	This study
RmP3150	RmP1629 with pTH2869 recombined into the chromosome	This study

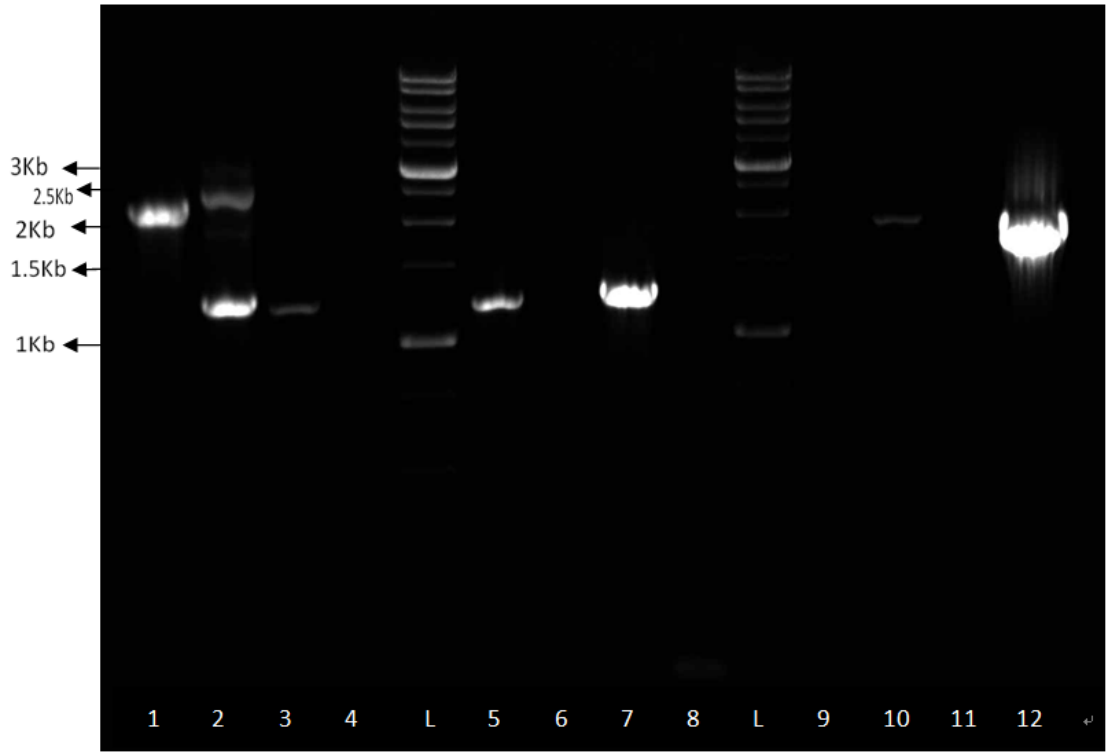

Figure 9. DNA agarose gel image showing the colony PCR product of RmP3149 and RmP3150 with different sets of primers. The genotype of the strains involved as well as expected number and size of the bands are specified in Figure 10 below. Lanes 1, 2 and 3 show colony PCR product of RmP3149 using primer sets 1, 2 and 3, respectively (Figure 10 (a)). Lanes 4 and 5 are colony PCR product of RmP3150 using primer sets 1 and 3 (Figure 10 (b)). Lane 6 and 7 are RmP1628 colony PCR using primer sets 1 and 2 (Figure 10 (c)). Lane 8 is RmP1629 colony PCR product using primer set 3. Lane 9, 10 and 11 are RmP110 colony PCR product using primer sets 1, 2 and 3 (Figure 10 (d)). Lane 12 is PCR product of *S. meliloti* genomic DNA amplified with primer set 2. Bands of expected number and sizes were observed on the gel.

(a) RmP3149

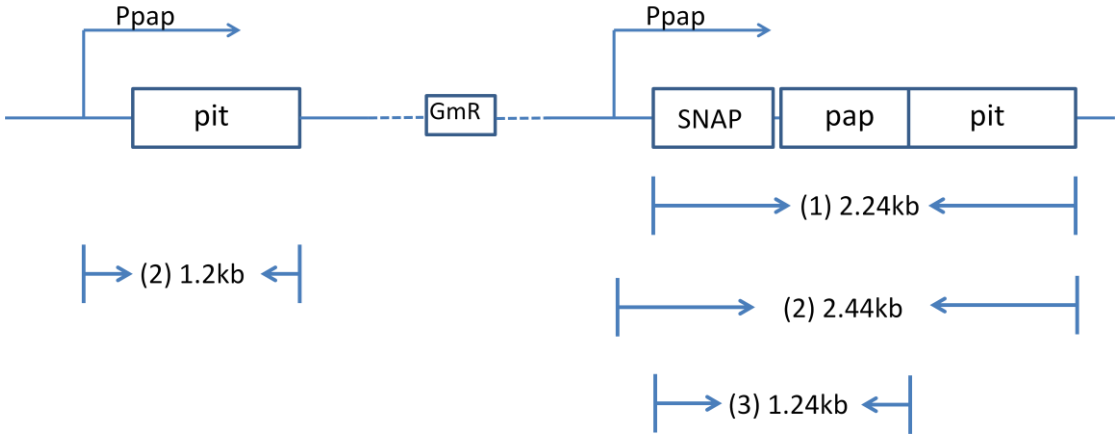

(b) RmP3150

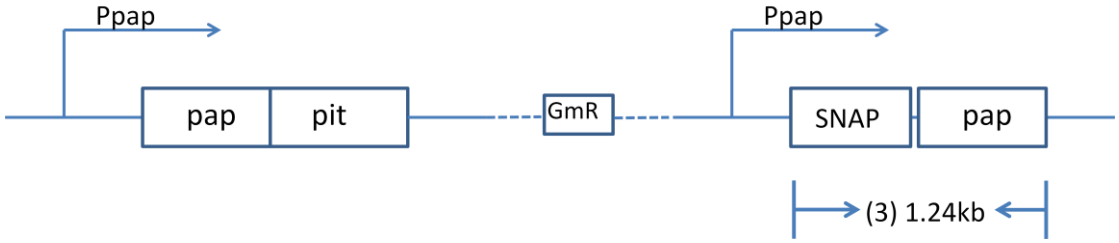

(c) RmP1628

(d) RmP110

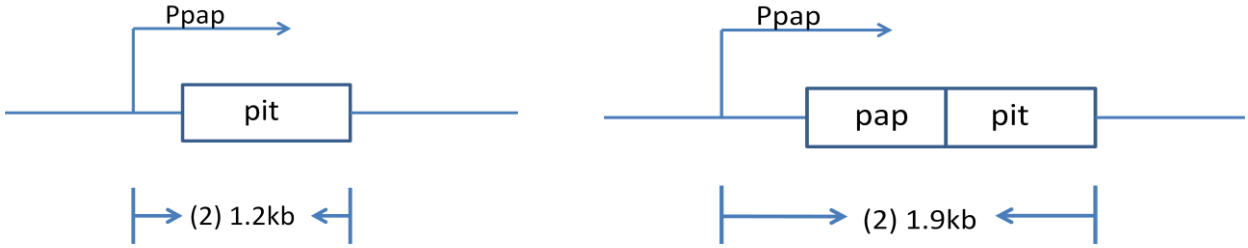

Figure 10. Expected sizes of RmP3149 and RmP3150 colony PCR products amplified with three different sets of primers (1), (2) and (3). Primer annealing sites and the expected sizes of PCR products in different strains are indicated in the chart. The primers that are unable to anneal with the template DNA are not included.

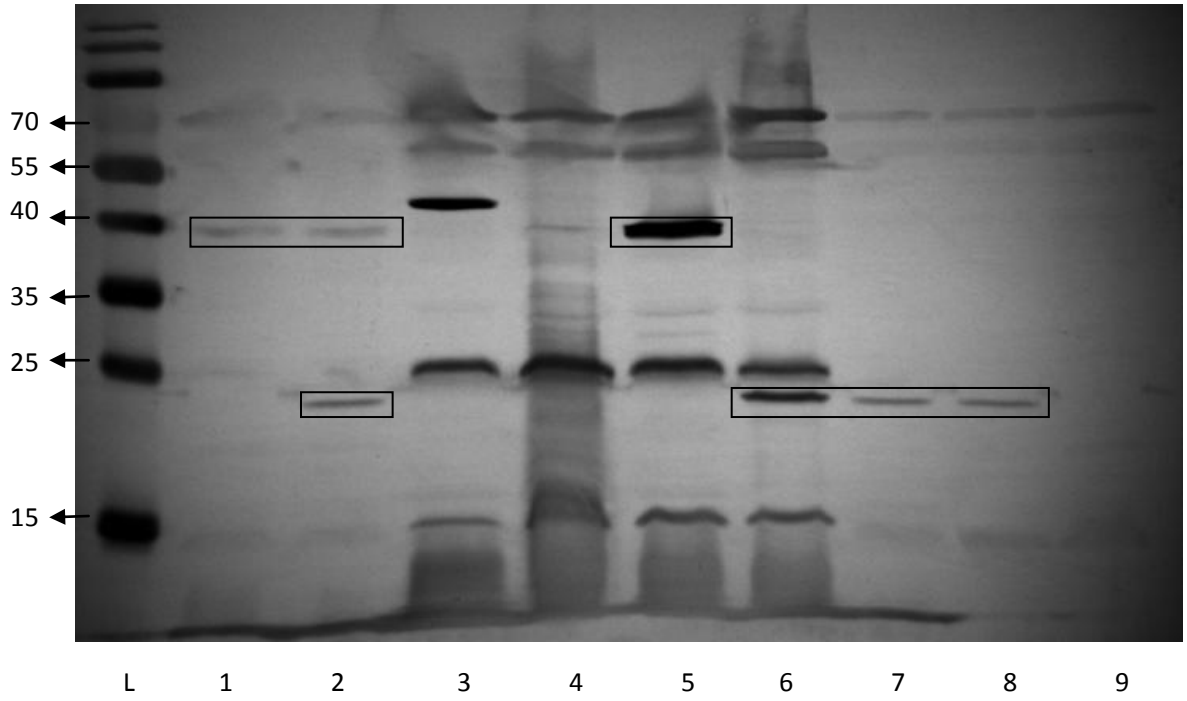

Figure 11. Western blot using Pap primary antibody to target Pap (23KD) and SNAP-Pap (~40KD) in the culture lysates. Lane 1 is cell lysate of RmP3149 which carries one copy of SNAP-*pap*. A band was detected at ~40KD indicating the presence of SNAP-Pap. Lane 2 is cell lysate of RmP3150 which carries one copy of SNAP-*pap* and one copy of wild type *pap*. Two bands appeared at 23KD and ~40KD respectively, indicating the expression of both SNAP-Pap and wild type Pap. Lane 3 and Lane 4 are MT2006 and MG1655 carrying pTH2869 which did not complement the *E. coli* mutants, correspondingly no Pap or SNAP-Pap signals were detected. Lane 5 is MG1655 carrying pTH2868 which complemented the *E. coli* mutants and SNAP-Pap could be seen at ~40KD. Lane 6 is MG1655 carrying pTH2825 (*S. meliloti pap-pit* in pUC118), wild type Pap was seen at 23KD. Lanes 7, 8 and 9 are RmP1629 (RmP110 *Δpit)*, RmP110 and RmP1628 (RmP110 *Δpap*), respectively. Wild type Pap could be seen in Lanes 7 and 8, but not in Lane 9.

Microscopy images showing Pap subcellular location

Superresolution microscopy pictures (Figure 12) show that the fluorescent signals are more intense toward the edge of the rod-shaped *E. coli* MT2016 carrying pTH2868. A couple of confocal microscope pictures (Figure 23) could be found in the *Appendix*.

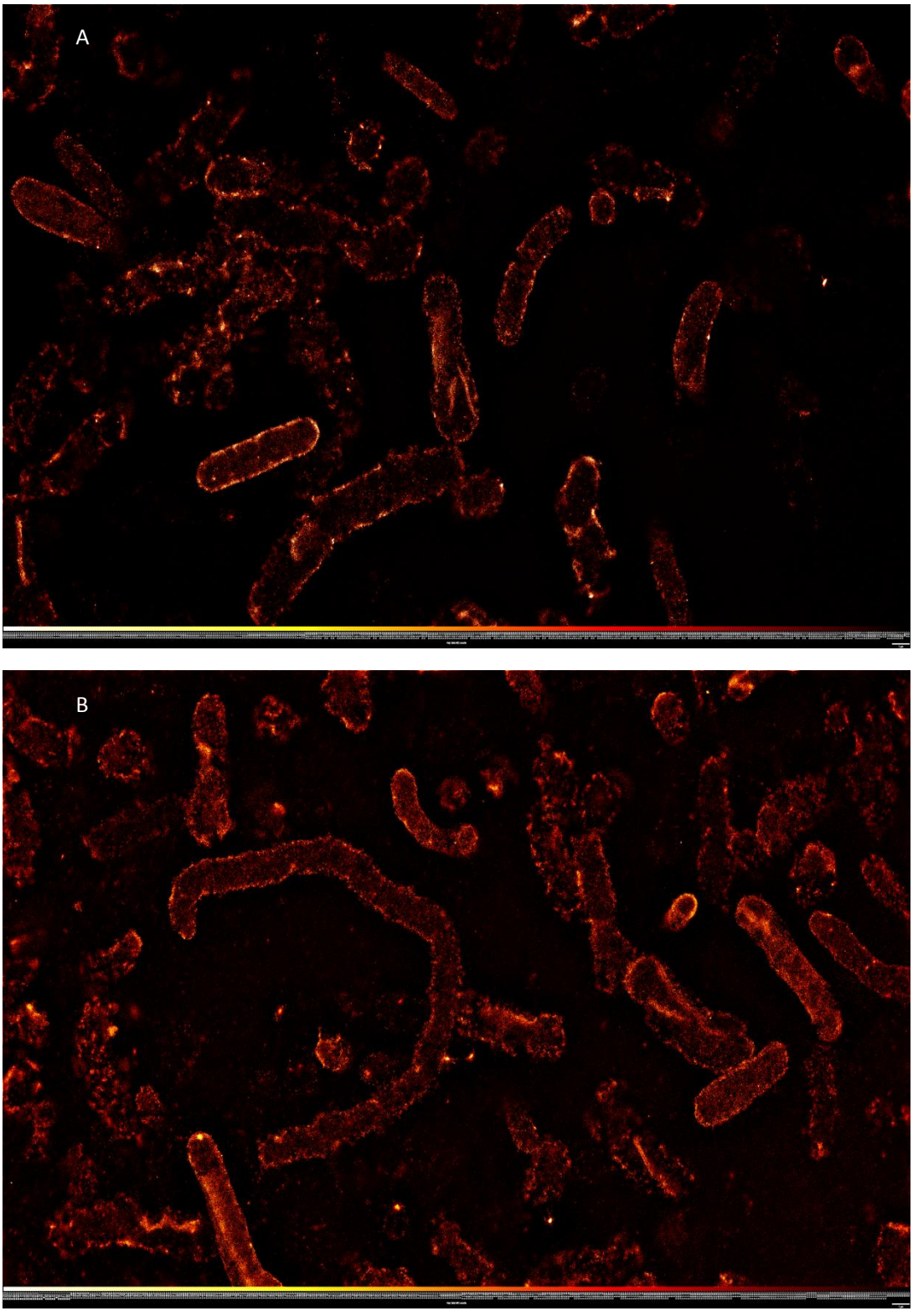

Figure 12. A and B are the two super-resolution microscopic images of MT2016 carrying pTH2868. pTH2868 is pUCP30T carrying SNAP-*pap-pit*, which complements the *E. coli* Pi uptake mutants. The fluorescent signals are more intense toward the edge of the cells and SNAP-Pap appears to be distributed close to the cell membrane. The white scale bar is at the right bottom corner of each picture indicating 1 μm.

pap-pit coding sequence region was deleted

S. meliloti pap-pit coding sequence region was deleted from RmP110 to construct the *pap-pit* deletion strain RmP3151. As can be seen in the left column of Figure 13, a fragment of only 1.2kb was amplified from RmP3151 as opposed to the 2.7kb PCR product which is 1.7kb *pap-pit* with its 500bp upstream and downstream regions amplified from RmP110. In the right column, the primers employed target the Kanamycin cassette. The Km cassette could not be amplified from RmP3151 but could be amplified from pKD13. The sequencing result shows the sequence of the scar of 107 nucleotides left over after the *pap-pit* deletion (Figure 14).

Complementation of the Δ*pap-pit* strain

After *phoB::TnV* was transduced into RmP3151 (RmP110 *Δpap-pit*) and RmP110, no transconjugants could be observed on the selective media for RmP3151, but there were about 70-80 tranductants for RmP110. For complementation, pTH2824 (*S. meliloti pap-pit* with 500 bp upstream and downstream regions in pUCP30T) , pTH2568 (*S. meliloti pit* in pTRsc) and pTH2569 (*S. meliloti pap-pit* in pTRsc) were conjugated into RmP3151 separately before *phoB::TnV* transduction, 50-60 transductants were recovered on each plate (Figure 15) for pTH2824 and pTH2569, but no colonies were observed for pTH2568 which only carries *pit*.

Table 5. Strains and plasmids involved in making *pap-pit* deletion strain

Plasmids and Strains	Description	References
plasmids		
pKD13	Template plasmid for Kanamycin cassette with FRT sites	Datsenko 2000
pKD46	temperature sensitive, arabinose inducible promoter for λ red recombinase, AmpR	Datsenko 2000
pUCP30T	ColEI *ori*V cloning vector, oriT, GmR,	Schweizer 1996
pTH1944	*flp* gene in a pBBR MCS-3 derivative with RK2-*tetR*-*tetA*, Tc^R	Milunovic 2011
pTH2824	*S. meliloti pap-pit* with 500bp upstream and downstream region of *pap-pit* cloned into pUCP30T	This study
pTH2897	Kanamycin cassette flanked by FRT sites and 500bp upstream and downstream region of *S. meliloti pap-pit* in pUCP30T	This study
***E. coli* strains**		
BW25113	rrnB3 DlacZ4787 hsdR514 D(araBAD)567 D(rhaBAD)568 rph-1	Datsenko 2000
M1420	BW25113 carrying pKD46	Lab stock
M842	DH5α carrying pTH1944	Lab stock
M2095	M1420 carrying pTH2824	This study
M2096	M1420 carrying pTH2897	This study
***S. meliloti* strains**		
RmP110	Rm1021 with changed wild-type *pstC*	Yuan 2006
RmP560	RcR2011 *phoB::TnV*	Lab stock
RmP3151	RmP110 *Δpap-pit*	This study

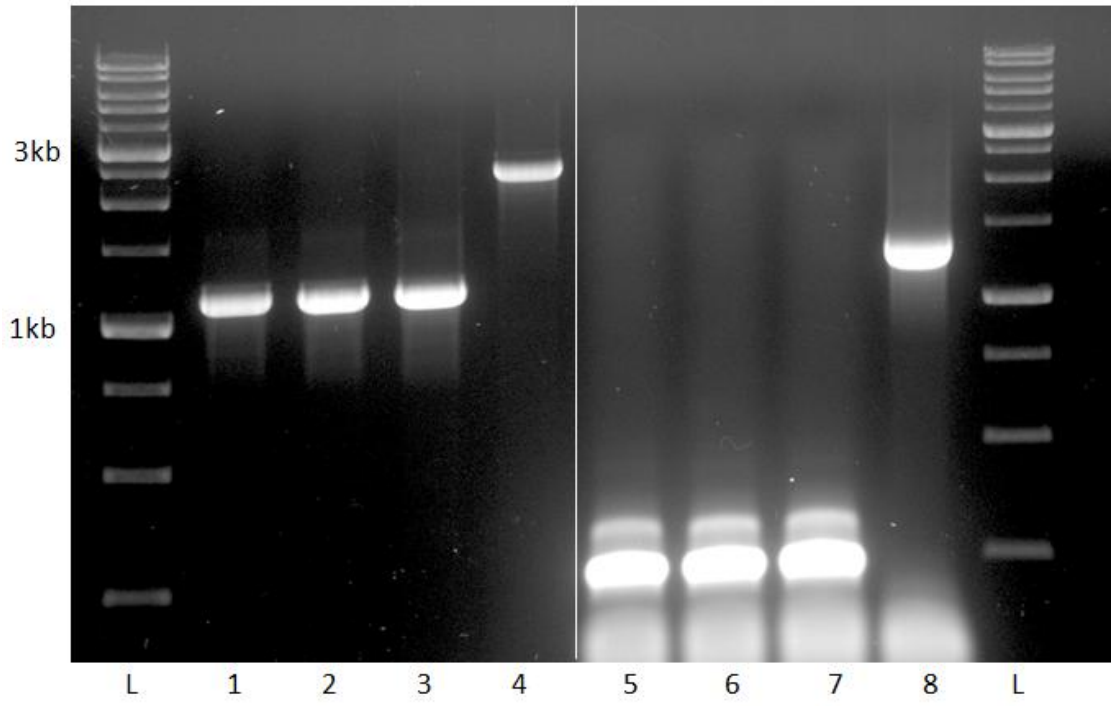

Figure 13. Colony PCR of RmP3151 and control strains amplified with two sets of primers. On the left column, all the colonies were amplified with the primers amplifying *pap-pit* and the 500bp upstream and downstream regions. Lane 1, 2 and 3 are PCR product of RmP3151 and show a band at 1.2kb in each lane. Lane 4 is RmP110 and shows a band at 2.7kb. On the right column, the colonies were amplified with primers targeting Km cassette. Lanes 5, 6 and 7 are PCR product of RmP3151. Lane 8 is PCR product of pKD13. A 1.4kb band was seen in the gel.

.....ACAATATGACAACTGCGTGACAATCGACAGTTGGATGGATCGCTG**GTGTAGGCTGGAGCTGCTTC**
GAAGTTCCTATACTTTCTAGAGAATAGGAACTTCGAACTGCAGGTCGACGGATCCCCGGAATTAATTC
TCATGTTTGACAGCTTATCCGCTTTCGCCGGGCACCCCGTTGGCATTGCCGGCGGCGGGGAGTATATTT
CCGCGATCTAATGGAATT.....

Figure 14. The *S. meliloti* nucleotide sequence after *pap-pit* deletion. The 107 nucleotides in bold are the scar left over after removing Km cassette by recombination between the flanking FRT sites. Underlined nucleotides are the upstream and downstream regions of *pap-pit*.

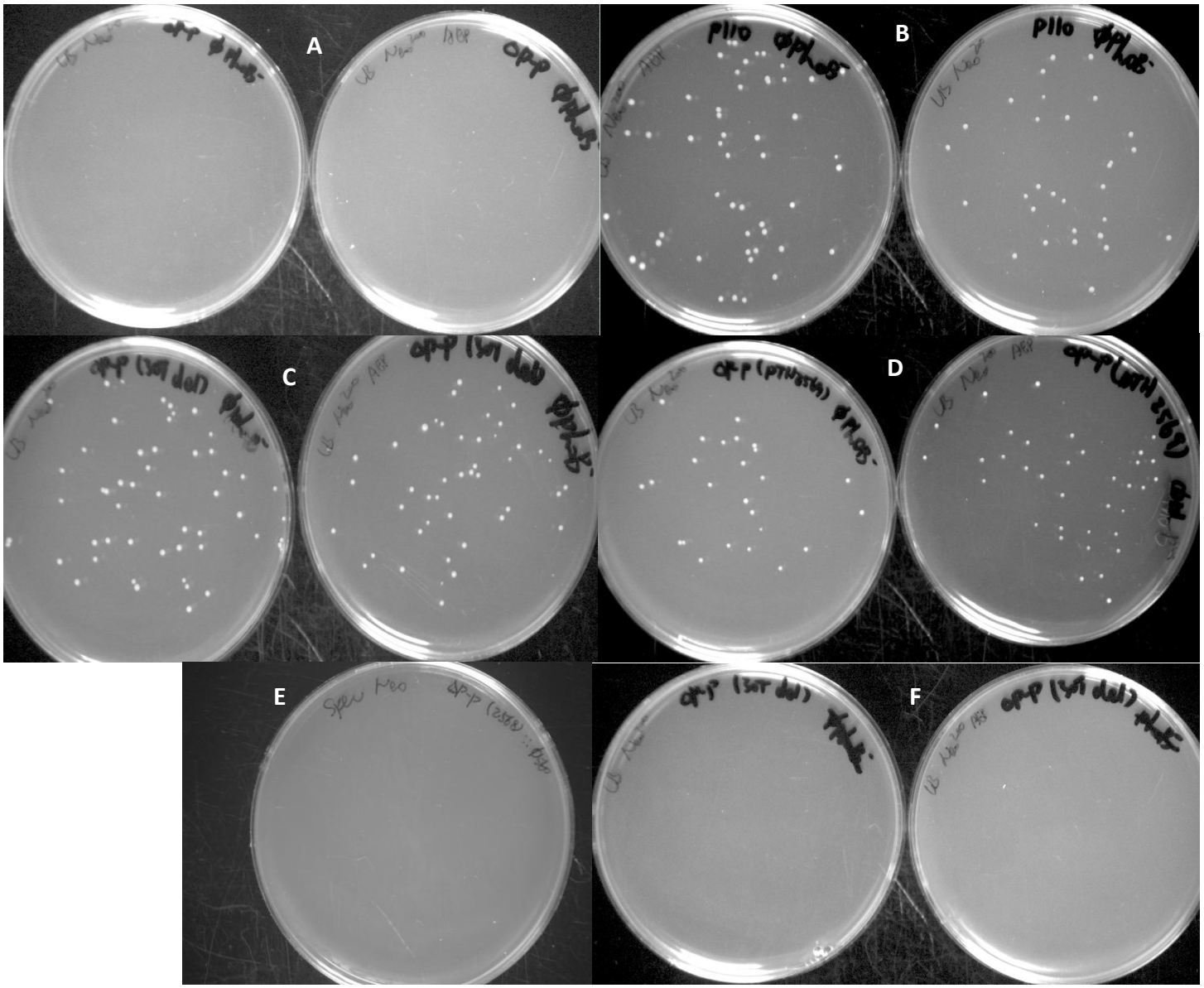

Figure 15. Complementation results of RmP3151. A) *PhoB::TnV* is transduced into RmP3151, no transductants could be recovered. B) *PhoB::TnV* is transduced into RmP110. Transductants were recovered. C) *PhoB::TnV* is transduced into RmP3151 with pTH2824 recombined into the chromosome, transductants were recovered; D) *PhoB::TnV* is transduced into RmP3151 carrying pTH2569 and transductants could be recovered; E) *PhoB::TnV* is transduced into RmP3151 carying pTH2568, no transductants were recovered; F) No-phage infection control. Just RmP3151 with pTH2824 recombined into the chromosome.

Discussion

Appropriate amount of Pap-Pit is important to its function

The coincidence of western blot result with complementation result of pTH2825, pTH2827, pTH2828 and pTH2569 (Figure 6) suggests that the failure of complementation is due to no or little Pap-Pit expression from the non-complementing plasmids. This also indicates that a minimum level of Pap and Pit is required for appropriate Pi uptake function.

Given the following facts of *S. meliloti pap-pit* clones:

a) *pap-pit* in **high** copy pUC118/119 vector **complemented** and **did not require IPTG** induction for complementation;

b) *pap-pit* in **medium** copy pTRsc vector **required IPTG** induction for complementation;

c) *pap-pit* in **low copy** pMW119 and pRK7813 vectors **did not complement**.

Since enough *S. meliloti* has been expressed from the high copy number plasmids pTH2825 and pTH2826, IPTG is not required in this case. However, IPTG is necessary for medium copy number plasmids pTH2569 to express sufficient level of Pap-Pit for complementation. And due to the extremely low copy number of pTH2827 and pTH2828 which did not complement, the resulting Pap-Pit amount was likely too little to complement no matter whether or not IPTG was added to the media. These results indicated the importance of Pap-Pit amount inside the cells.

Given following facts for *S. oneidensis pap-pit* clones*:*

a) *pap-pit* in **medium** copy pTRsc complemented without IPTG, but was **lethal** when IPTG was added to the media.

b) *pap-pit* in **low** copy pMW119 **complemented** and **did not require IPTG**.

Since *S. oneidensis* is phylogenetically closer to *E. coli* (both are gamma-proteobacteria, Gram negative), *pit* from this organism might be more compatible, active and potent in *E. coli* than *S.meliloti pit* and *S.coelicolor pitH1*. Therefore, when *S. oneidensis* Pap-Pit is expressed *in trans* in the *E. coli* mutants, much smaller amounts are needed for complementation, and too much expression will even inhibit the cell growth. Accordingly, when *S. oneidensis* Pap-Pit is expressed from the low copy number vector pMW119, it complemented the mutants very nicely, independent of IPTG addition. However, when cloned into medium copy number vector pTRsc, *S. oneidensis pap-pit* complemented without IPTG, and the overexpression of it inhibited the cell growth, including the wild type. This indicated that there is an optimal level of Pap- Pit and an excess amount of it can be toxic to the host cells. There can be many possible reasons for this toxicity, including too much cell energy consumption by the transport process and excess intracellular Pi accumulation.

Based on the analysis above, appropriate amounts of Pap-Pit seem very important to its function. Too much Pap-Pit inhibits the growth, while too little does not make any difference from empty vectors.

Pap may serve to optimize Pit function by

Improving Pit efficiency in response to insufficient Pit

When comparing pTH2872 (*S. oneidensis pap-pit* in pTRsc) and pTH2873 (*S. oneidensis pit* in pTRsc), it can be seen that *S. oneidensis pit* alone only showed poor complementation and even this required IPTG induction, while *pap-pit* together showed optimal complementation. The hypothesis is that Pap can improve Pit efficiency by stabilizing Pit protein or transcript or by interacting with it to increase its activity in the recognition, binding or transporting of the substrate Pi.

Alleviating toxicity of excess PitH1

Given the Important facts for *S. coelicolor*:

a) pTH2631 (*pitH1* in pTRsc) complemented without IPTG, but was lethal with IPTG;
b) pTH2864 (*pap* in pUC119) did not complement;
c) pTH2631 and pTH2864 together were no longer lethal to the cells and complemented the mutants with IPTG.

As described above, the inhibition caused by pTH2631 could be alleviated by pTH2864. Therefore, Pap was speculated to be able to eliminate the toxicity of excess PitH1. This might be achieved by doing something opposite to what it does in response to insufficient Pit as discussed above. That is, it might reduce PitH1 amount, stability or activity in this case. This also explained why IPTG induction was required

for complementation when pTH2864 was together with pTH2631 inside the cells: Since Pap expressed from pTH2864 (high copy number plasmid) significantly reduced the amount or activity of PitH1 from pTH2631 (medium copy number plasmid), IPTG is required to compensate for the lower amount or activity of PitH1 compared with pTH2631 alone for complementation.

The two aspects discussed above suggest that Pap might optimize Pit functioning in response to Pit content, which on one hand maintains enough Pi intracellular concentration, on the other hand reduces the risk of toxicity to the cells for bacterial survival.

Eliminating mucoid phenotype

The difference between *S. meliloti pap-pit* and *pit* alone can be illustrated by comparing pTH2569 (*S. meliloti pap-pit* in pTRsc) and pTH2568 (*S. meliloti pit* in pTRsc). It can be seen that the *E. coli* mutants expressing *S. meliloti* Pit alone exhibited a mucoid phenotype which might have been resulted from capsule formation, but the presence of Pap was able to eliminate the mucoid phenotype which is abnormal for the *E. coli* strains employed in this study.

Inhibiting PhoB which negatively regulates Pap-Pit system

As mentioned in the *introduction*, PhoU_div, which is the single domain in Pap, is a member of PhoU-like superfamily apart from PhoU family. There are some other connections between PhoU and PhoU_div as specified in the *Introduction*. Therefore,

Pap and PhoU might share some similar regulatory mechanisms. Since PhoU is the chaperone-like PhoR/PhoB inhibitory protein in PstSCAB–PhoU system, as an analogue to PhoU, Pap might play a similar role in Pap-Pit system as PhoU does in PstSCAB. In Pap-Pit system, PhoB is the negative regulator and Pap may inhibit PhoB to reduce its repression effect on *pap-pit*.

Conserved amino acids are considered functionally important in Pap

The conserved amino acids were considered functionally important and the prediction appears reliable since they are not randomly distributed but instead form three patches. In addition, the three patches all exist on one face of the molecule although the two faces are nearly geometrically symmetric. Besides, 7 out of the 11 conserved surface amino acids are polar acidic (D and E), so the conserved patches tend to be negatively charged and hydrophilic and may bind to positively charged metal ions while assisting the transport of phosphate. A conserved motif E/DXXXD was described as being the iron cluster binding motif in PhoU family in Pfam database (Punta, Coggill et al. 2012). Likewise, among the highly conserved amino acids identified in Pap, the E/DXXXD motif occurred seven times in total in the protein and five out of the seven involve the highly conserved amino acids. Futher, all the conserved polar amino acids D and E are only present in this motif.

SNAP-Pap is expressed as a fusion protein; SNAP fusion appears to compromise Pap activity in *S. meliloti*

The presence of RmP3149/RmP3150 PCR product of expected sizes using primers targeting SNAP gene suggests that pTH2869 has been recombined into the chromosome of RmP1628 and RmP1629. Western blot results suggest that SNAP-*pap* gene can be expressed in RmP3149 and RmP3150 as a fusion protein, indicated by the shift of Pap from 23KD to ~40KD. As for the complementation experiment involving RmP3149 and RmP3150, a possible explanation for the failure of complementation of RmP3149 is that RmP3149 only has SNAP-*pap* but not the wild type *pap,* whereas RmP3150 still has one copy of wild type *pap-pit* in addition to SNAP-*pap* (Figure 10). This indicates that, unlike in *E. coli*, Pap activity might have been lost or significantly reduced when it has the SNAP tag at the N-terminus in *S. meliloti.* It also proves that Pap is an indispensable part in *S. meliloti* strains defective in all other phosphate transporters.

SNAP-Pap is located along the cell membrane intracellularly in *E. coli*

The ability of pTH2868 (SNAP-*pap-pit* in pUCP30T) to complement the *E. coli* Pi uptake mutants MT2006 and MT2016 indicated that Pap-Pit is still functional in the *E. coli* strains in spite of the presence of the 182-amino-acid SNAP tag. The correct localization of Pap with SNAP-tag is presumably essential to Pap function and Pap-Pit interaction. Therefore, cells carrying this plasmid were later used for fluorescent

microscopy to determine the localization of Pap. pTH2869 did not appear to complement probably due to the low expression level of SNAP-Pap-Pit because its expression from pTH2869 is driven by native *S. meliloti* Pap promoter instead of P*lac* in pTH2868.

The SNAP fluorescent signals showed that Pap is distributed along the membrane in the cytoplasm. This might suggest that Pap may act on Pit through physical interaction.

pap-pit has been successfully deleted

Colony PCR and sequencing result indicated the successful deletion of *pap-pit* from RmP110. The transduction of *PhoB::TnV* into RmP3151 (RmP110 *Δpap-pit*) failed to form any colonies, which is expected as the transductants are not able to uptake Pi due to the inactivated PstSCAB system and PhnCDET system as well as the deleted *pap-pit*. The ability of pTH2569/pTH2824 and the inability of pTH2568 to complement RmP3151 again proved the importance of Pap in Pap-Pit system function. Since RmP3151ϕ*PhoB::TnV* transductants cannot be recovered on the selective media but the growth deficiency can be complemented by a specific plasmid, RmP3151 can be used as the background strain to test the ability of the plasmid carrying *pap* with mutagenized amino acids identified to complement RmP3151 in order to determine the key amino acids in Pap.

References

Ahmad, S., M. Gromiha, H. Fawareh and A. Sarai (2004). "ASAView: Database and tool for solvent accessibility representation in proteins." BMC Bioinformatics **5**(1): 51.

Armon, A., D. Graur and N. Ben-Tal (2001). "ConSurf: an algorithmic tool for the identification of functional regions in proteins by surface mapping of phylogenetic information." J Mol Biol **307**(1): 447-463.

Bardin, S., S. Dan, M. Osteras and T. M. Finan (1996). "A phosphate transport system is required for symbiotic nitrogen fixation by Rhizobium meliloti." J Bacteriol **178**(15): 4540-4547.

Bardin, S. D., R. T. Voegele and T. M. Finan (1998). "Phosphate Assimilation in Rhizobium(Sinorhizobium) meliloti: Identification of apit-Like Gene." Journal of Bacteriology **180**(16): 4219-4226.

Bertani, G. (1952). "Studies on Lysogenesis. I. The mode of phage liberation by lysogenic Escherichia coli." J. of Bacteriology **62**: 293-300.

Bieleski, R. L. (1973). "Phosphate Pools, Phosphate Transport, and Phosphate Availability." Annual Review of Plant Physiology **24**(1): 225-252.

Datsenko, K. A. and B. L. Wanner (2000). "One-step inactivation of chromosomal genes in Escherichia coli K-12 using PCR products." Proceedings of the National Academy of Sciences **97**(12): 6640-6645.

Davidson, A. L. and J. Chen (2004). "ATP-BINDING CASSETTE TRANSPORTERS IN BACTERIA." Annual Review of Biochemistry **73**(1): 241-268.

Davidson, A. L., E. Dassa, C. Orelle and J. Chen (2008). "Structure, Function, and Evolution of Bacterial ATP-Binding Cassette Systems." Microbiology and Molecular Biology Reviews **72**(2): 317-364.

Edgar, R. C. (2004). "MUSCLE: multiple sequence alignment with high accuracy and high throughput." Nucleic Acids Res **32**(5): 1792-1797.

Elias, A. O., M. J. Abarca, R. A. Montes, T. G. Chasteen, J. M. Perez-Donoso and C. C. Vasquez (2012). "Tellurite enters Escherichia coli mainly through the PitA phosphate transporter." Microbiologyopen **1**(3): 259-267.

Finn, R. D., J. Clements and S. R. Eddy (2011). "HMMER web server: interactive sequence similarity searching." Nucleic Acids Research **39**(suppl 2): W29-W37.

Hanahan, D. (1983). "Studies on transformation of Escherichia coli with plasmids." J Mol Biol **166**(4): 557-580.

Harris, R. M., D. C. Webb, S. M. Howitt and G. B. Cox (2001). "Characterization of PitA and PitB fromEscherichia coli." Journal of Bacteriology **183**(17): 5008-5014.

Hollenstein, K., D. C. Frei and K. P. Locher (2007). "Structure of an ABC transporter in complex with its binding protein." Nature **446**(7132): 213-216.

Hsieh, Y. J. and B. L. Wanner (2010). "Global regulation by the seven-component Pi signaling system." Curr Opin Microbiol **13**(2): 198-203.

Huang, Y., M. J. Lemieux, J. Song, M. Auer and D.-N. Wang (2003). "Structure and Mechanism of the Glycerol-3-Phosphate Transporter from Escherichia coli." Science **301**(5633): 616-620.

Jain, E., A. Bairoch, S. Duvaud, I. Phan, N. Redaschi, B. E. Suzek, M. J. Martin, P. McGarvey and E. Gasteiger (2009). "Infrastructure for the life sciences: design and implementation of the UniProt website." BMC Bioinformatics **10**: 136.

Jones, J. D. G. and N. Gutterson (1987). "An efficient mobilizable cosmid vector, pRK7813, and its use

in a rapid method for marker exchange in Pseudomonas fluorescens strain HV37a." Gene **61**(3): 299-306.

Keppler, A., H. Pick, C. Arrivoli, H. Vogel and K. Johnsson (2004). "Labeling of fusion proteins with synthetic fluorophores in live cells." Proceedings of the National Academy of Sciences of the United States of America **101**(27): 9955-9959.

Lamarche, M. G., B. L. Wanner, S. Crepin and J. Harel (2008). "The phosphate regulon and bacterial virulence: a regulatory network connecting phosphate homeostasis and pathogenesis." FEMS Microbiol Rev **32**(3): 461-473.

Law, C. J., P. C. Maloney and D.-N. Wang (2008). "Ins and Outs of Major Facilitator Superfamily Antiporters." Annual Review of Microbiology **62**(1): 289-305.

Liu, J., Y. Lou, H. Yokota, P. D. Adams, R. Kim and S. H. Kim (2005). "Crystal structure of a PhoU protein homologue: a new class of metalloprotein containing multinuclear iron clusters." J Biol Chem **280**(16): 15960-15966.

Locher, K. P., A. T. Lee and D. C. Rees (2002). "The E. coli BtuCD Structure: A Framework for ABC Transporter Architecture and Mechanism." Science **296**(5570): 1091-1098.

Long, S. R. (2001). "Genes and Signals in the Rhizobium-Legume Symbiosis." Plant Physiology **125**(1): 69-72.

Motomura, K., R. Hirota, N. Ohnaka, M. Okada, T. Ikeda, T. Morohoshi, H. Ohtake and A. Kuroda (2011). "Overproduction of YjbB reduces the level of polyphosphate in Escherichia coli: a hypothetical role of YjbB in phosphate export and polyphosphate accumulation." FEMS Microbiol Lett **320**(1): 25-32.

Oganesyan, V., N. Oganesyan, P. D. Adams, J. Jancarik, H. A. Yokota, R. Kim and S. H. Kim (2005). "Crystal structure of the "PhoU-like" phosphate uptake regulator from Aquifex aeolicus." J Bacteriol **187**(12): 4238-4244.

Pao, S. S., I. T. Paulsen and M. H. Saier (1998). "Major Facilitator Superfamily." Microbiology and Molecular Biology Reviews **62**(1): 1-34.

Punta, M., P. C. Coggill, R. Y. Eberhardt, J. Mistry, J. Tate, C. Boursnell, N. Pang, K. Forslund, G. Ceric, J. Clements, A. Heger, L. Holm, E. L. L. Sonnhammer, S. R. Eddy, A. Bateman and R. D. Finn (2012). "The Pfam protein families database." Nucleic Acids Research **40**(D1): D290-D301.

Rees, D. C., E. Johnson and O. Lewinson (2009). "ABC transporters: the power to change." Nat Rev Mol Cell Biol **10**(3): 218-227.

Rosenberg, H., R. G. Gerdes and K. Chegwidden (1977). "Two systems for the uptake of phosphate in Escherichia coli." Journal of Bacteriology **131**(2): 505-511.

Saier, M. H., Jr., J. T. Beatty, A. Goffeau, K. T. Harley, W. H. Heijne, S. C. Huang, D. L. Jack, P. S. Jahn, K. Lew, J. Liu, S. S. Pao, I. T. Paulsen, T. T. Tseng and P. S. Virk (1999). "The major facilitator superfamily." J Mol Microbiol Biotechnol **1**(2): 257-279.

Sambrook, J. a. R., D. W. (2001). Molecular cloning : a laboratory manual 3rd ed, CSHL Press.

Schwede, T., J. Kopp, N. Guex and M. C. Peitsch (2003). "SWISS-MODEL: an automated protein homology-modeling server." Nucleic Acids Research **31**(13): 3381-3385.

Voegele, R. T., S. Bardin and T. M. Finan (1997). "Characterization of the Rhizobium (Sinorhizobium) meliloti high- and low-affinity phosphate uptake systems." Journal of Bacteriology **179**(23): 7226-7232.

Wanner, B. L. and W. W. Metcalf (1992). "Molecular genetic studies of a 10.9-kb operon in Escherichia coli for phosphonate uptake and biodegradation." FEMS Microbiol Lett **79**(1-3): 133-139.

Ward, A., C. L. Reyes, J. Yu, C. B. Roth and G. Chang (2007). "Flexibility in the ABC transporter MsbA:

Alternating access with a twist." Proceedings of the National Academy of Sciences **104**(48): 19005-19010.

Yuan, Z.-C., R. Zaheer and T. M. Finan (2006). "Regulation and Properties of PstSCAB, a High-Affinity, High-Velocity Phosphate Transport System of Sinorhizobium meliloti." Journal of Bacteriology **188**(3): 1089-1102.

Yuan, Z.-C., R. Zaheer, R. Morton and T. M. Finan (2006). "Genome prediction of PhoB regulated promoters in Sinorhizobium meliloti and twelve proteobacteria." Nucleic Acids Research **34**(9): 2686-2697.

Appendix

```
   1 AGATTGCAGC ATTACACGTC TTGAGCGATT GTGTAGGCTG GAGCTGCTTC GAAGTTCCTA
  61 TACTTTCTAG AGAATAGGAA CTTCGGAATA GGAACTTCAA GATCCCCTTA TTAGAAGAAC
 121 TCGTCAAGAA GGCGATAGAA GGCGATGCGC TGCGAATCGG GAGCGGCGAT ACCGTAAAGC
 181 ACGAGGAAGC GGTCAGCCCA TTCGCCGCCA AGCTCTTCAG CAATATCACG GGTAGCCAAC
 241 GCTATGTCCT GATAGCGGTC CGCCACACCC AGCCGGCCAC AGTCGATGAA TCCAGAAAAG
 301 CGGCCATTTT CCACCATGAT ATTCGGCAAG CAGGCATCGC CATGGGTCAC GACGAGATCC
 361 TCGCCGTCGG GCATGCGCGC CTTGAGCCTG GCGAACAGTT CGGCTGGCGC GAGCCCCTGA
 421 TGCTCTTCGT CCAGATCATC CTGATCGACA AGACCGGCTT CCATCCGAGT ACGTGCTCGC
 481 TCGATGCGAT GTTTCGCTTG GTGGTCGAAT GGGCAGGTAG CCGGATCAAG CGTATGCAGC
 541 CGCCGCATTG CATCAGCCAT GATGGATACT TTCTCGGCAG GAGCAAGGTG AGATGACAGG
 601 AGATCCTGCC CCGGCACTTC GCCCAATAGC AGCCAGTCCC TTCCCGCTTC AGTGACAACG
 661 TCGAGCACAG CTGCGCAAGG AACGCCCGTC GTGGCCAGCC ACGATAGCCG CGCTGCCTCG
 721 TCCTGCAGTT CATTCAGGGC ACCGGACAGG TCGGTCTTGA CAAAAAGAAC CGGGCGCCCC
 781 TGCGCTGACA GCCGGAACAC GGCGGCATCA GAGCAGCCGA TTGTCTGTTG TGCCCAGTCA
 841 TAGCCGAATA GCCTCTCCAC CCAAGCGGCC GGAGAACCTG CGTGCAATCC ATCTTGTTCA
 901 ATCATGCGAA ACGATCCTCA TCCTGTCTCT TGATCAGATC TTGATCCCCT GCGCCATCAG
 961 ATCCTTGGCG GCAAGAAAGC CATCCAGTTT ACTTTGCAGG GCTTCCCAAC CTTACCAGAG
1021 GGCGCCCCAG CTGGCAATTC CGGTTCGCTT GCTGTCCATA AAACCGCCCA GTCTAGCTAT
1081 CGCCATGTAA GCCCACTGCA AGCTACCTGC TTTCTCTTTG CGCTTGCGTT TTCCCTTGTC
1141 CAGATAGCCC AGTAGCTGAC ATTCATCCGG GGTCAGCACC GTTTCTGCGG ACTGGCTTTC
1201 TACGTGTTCC GCTTCCTTTA GCAGCCCTTG CGCCCTGAGT GCTTGCGGCA GCGTGAGCTT
1261 CAAAAGCGCT CTGAAGTTCC TATACTTTCT AGAGAATAGG AACTTCGAAC TGCAGGTCGA
1321 CGGATCCCCG GAATTAATTC TCATGTTTGA CAGCTTATCA CTGATCAGTG AATTAATGGC
1381 GATGACGCAT CCTCACGATA ATATCCGGGT AGGCGCAATC ACTTTCGTCT CTACTCCGTT
1441 ACAAAGCGAG GCTGGGTATT TCCCGGCCTT TCTGTTATCC GAAATCCACT GAAAGCACAG
```

Figure 16. pKD13 sequence. The priming sites are underlined with solid line. FRT sites are the shaded sequences and Kanamycin gene open reading frame is underlined with dotted line.

Complementation results:

The complementation of the plasmids for the mutants is shown by the images below. The plates in each set are labeled as M9, M9/IPTG, M9/G3P and M9/I/G (M9 containing both G3P and IPTG). Each plate is divided into two sections by a red line. The three strains (mutants MT2006, MT2016 and the wild type MG1655) carrying the specific plasmid are in the larger section with the two mutants carrying the plasmid on the top. The same strains without the plasmid are in the smaller section with the two mutants on the right and the wild type on the left. There are specific descriptions for the plates with a different pattern.

S. meliloti complementation results

pTH2825 (pUC118 carrying *S. meliloti pap-pit* from pTH348) complement (++)

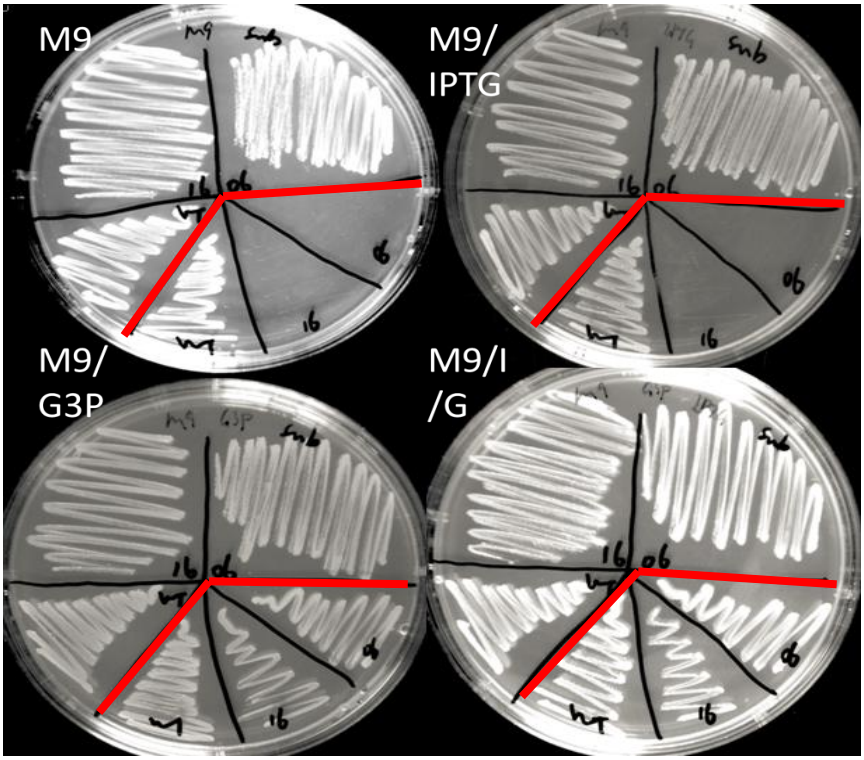

pTH2826 (*S. meliloti pap-pit* in pUC119) complement (++). A duplicate was included for MT2016 carrying the plasmid.

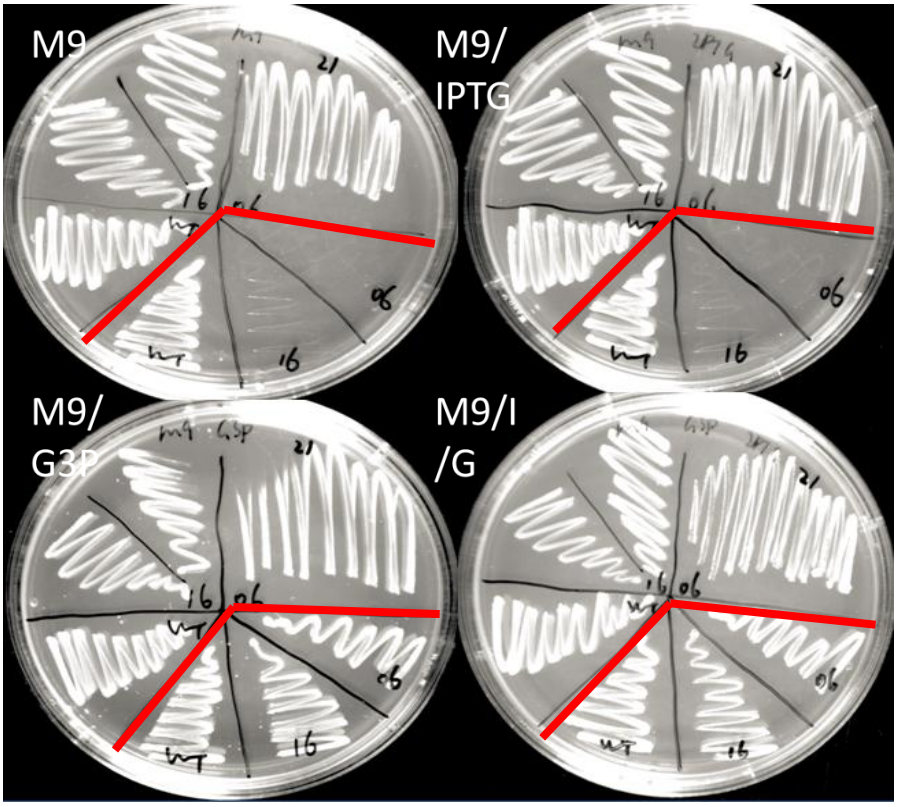

pTH2569 (*S. meliloti pap-pit* in pTRsc) complement on M9/IPTG (++)

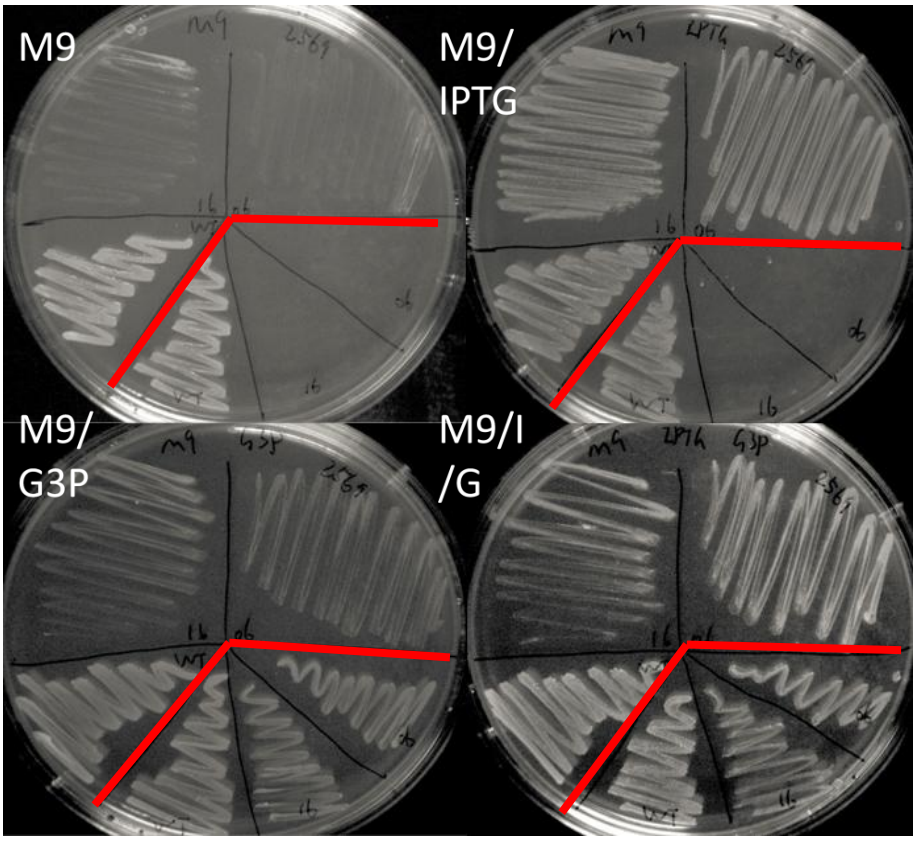

pTH2568 (*S.meliloti pit* in pTRsc) formed mucoid colonies when IPTG is present.

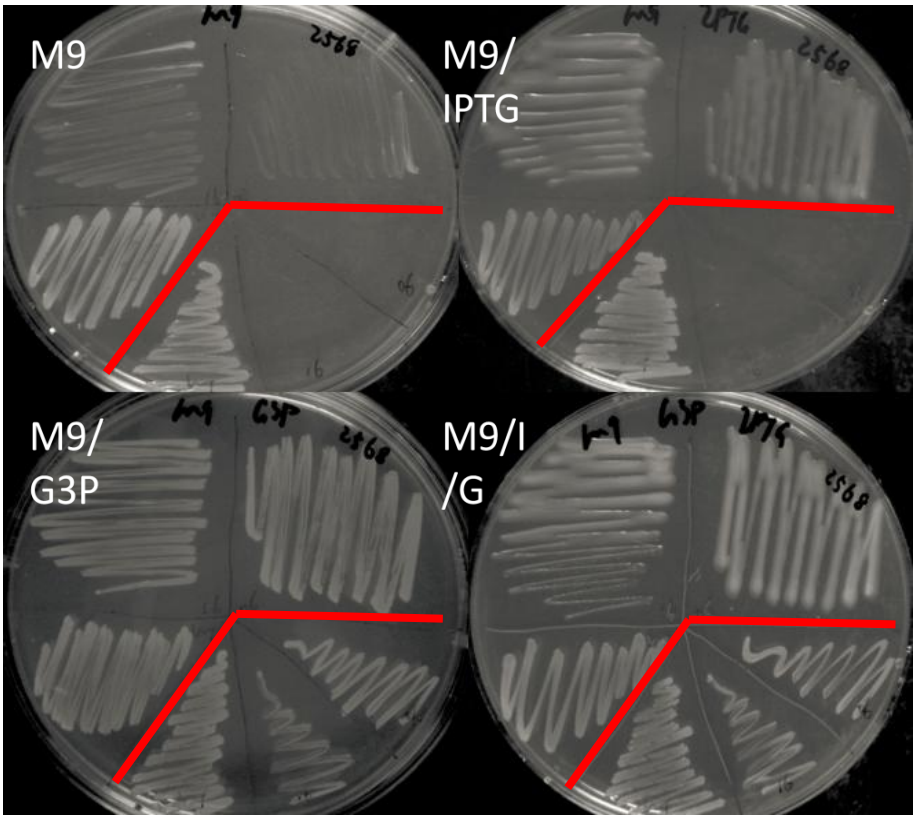

pTH2829 (*S.meliloti pit* in pMW119) didn't complement. In this set, MT2006 and MT2016 carrying this plasmid are on the top region, and MT2006, MT2016 and MG1655 without the plasmid are in the region below. MG1655 carrying the plasmid is omitted.

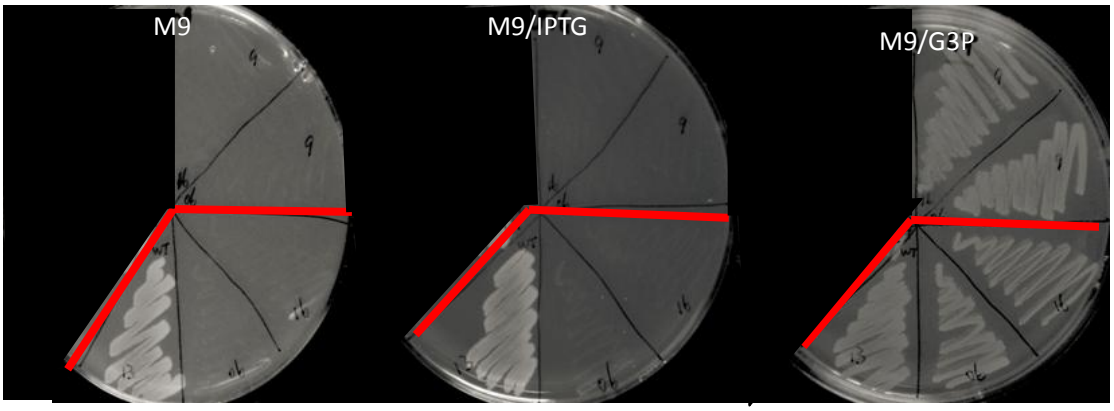

pTH2567 (*S. meliloti pap* in pTRsc) didn't complement.

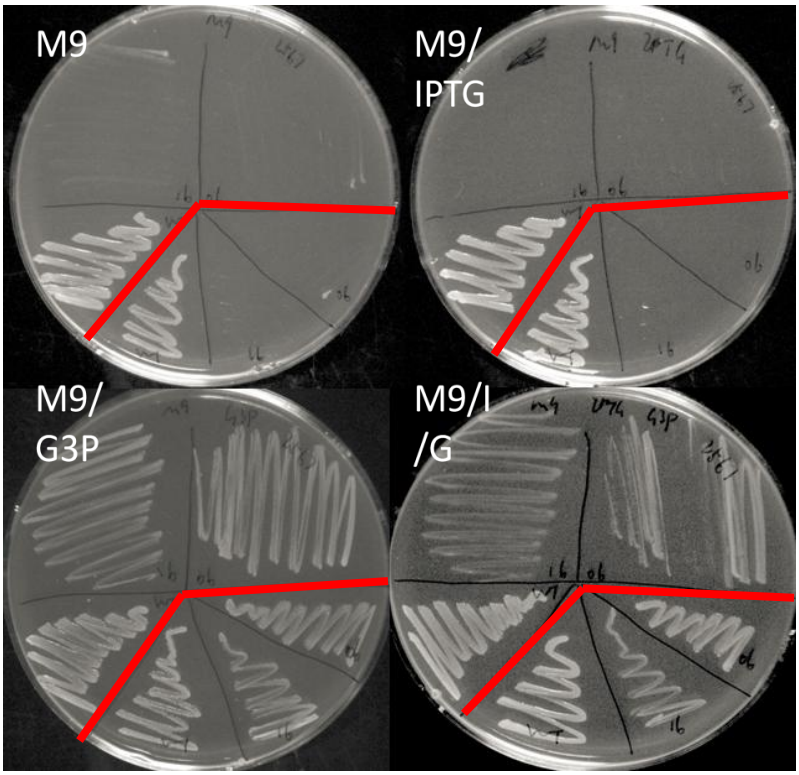

S. oneidensis complementation result

pTH2871 (*S. oneidensis pap-pit* in pTRsc) complement on M9 (++) but is lethal on M9/IPTG.

Duplicates are included for MT2016 carrying the plasmid.

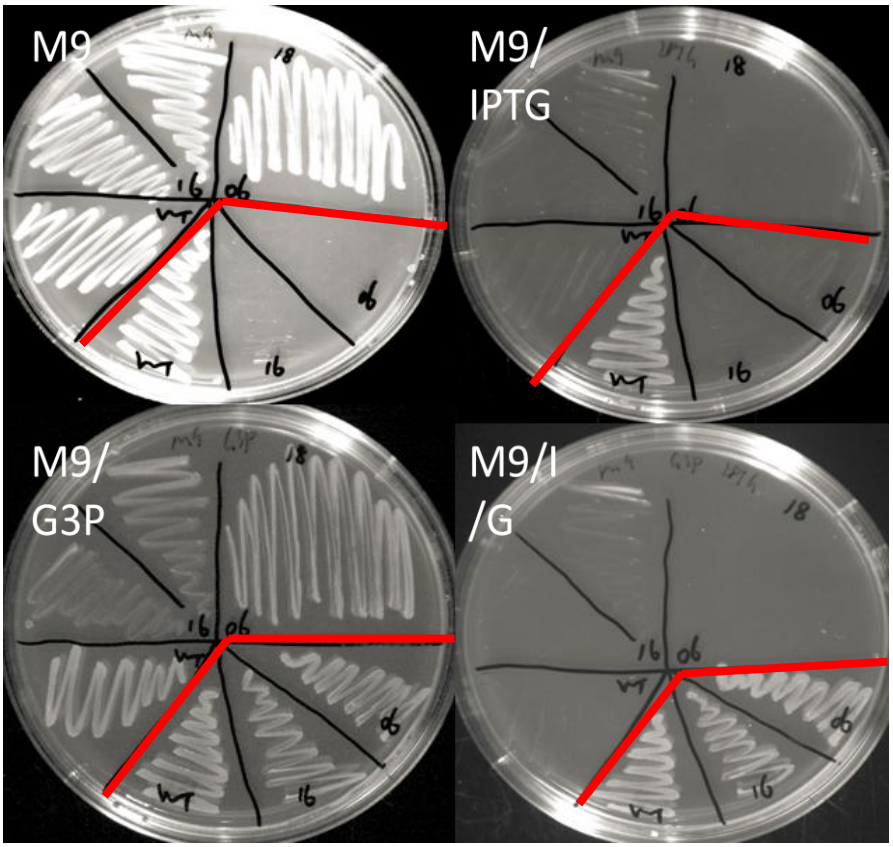

pTH2872 (*S. oneidensis pap-pit* in pMW119) complemented (++)

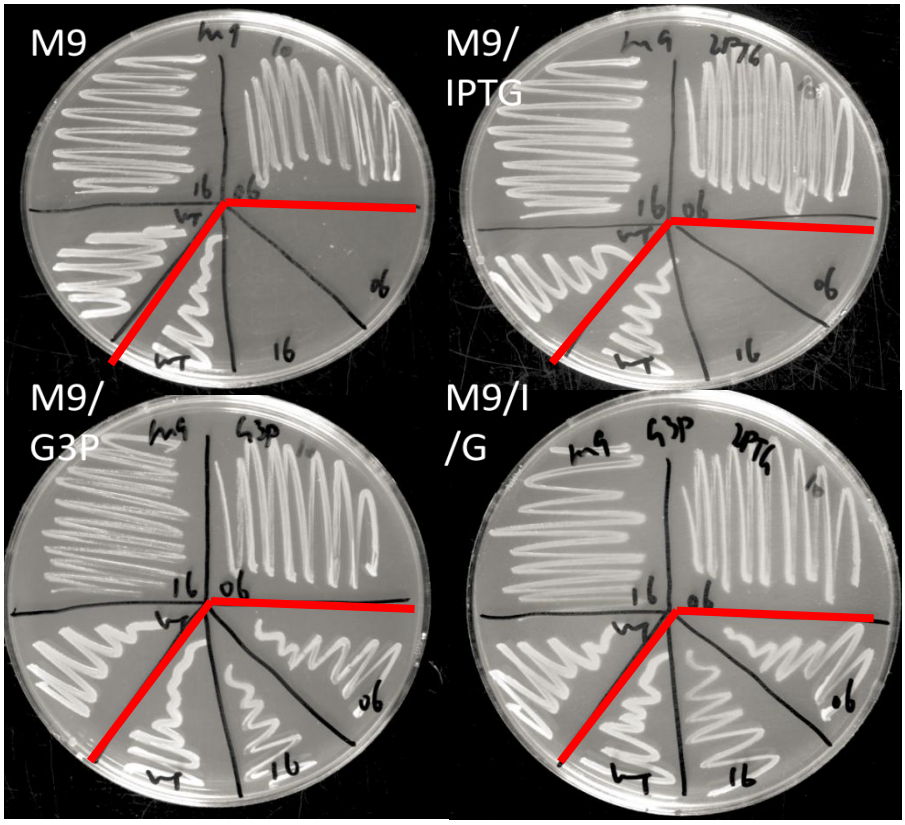

pTH2873 (*S. oneidensis pit* in pMW119) complement on M9/IPTG (+). In the top left section are the three strains carrying the plasmid. In the bottom right section are the strains without the plasmid.

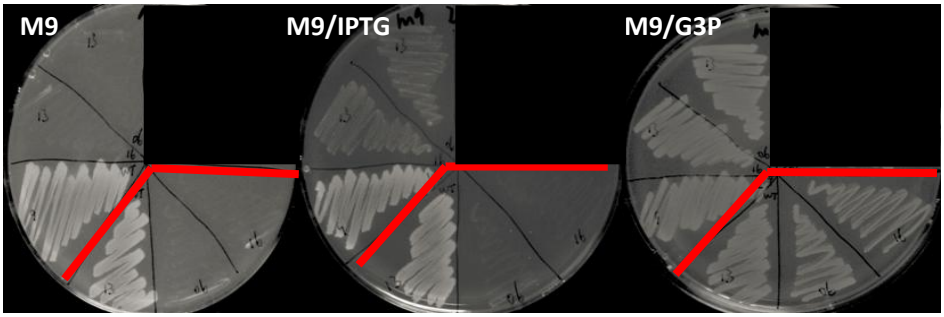

pTH2863 (*S. oneidensis pap* in pTRsc) complement slightly on M9, also a little bit on M9/IPTG, perhaps because of pTRsc.

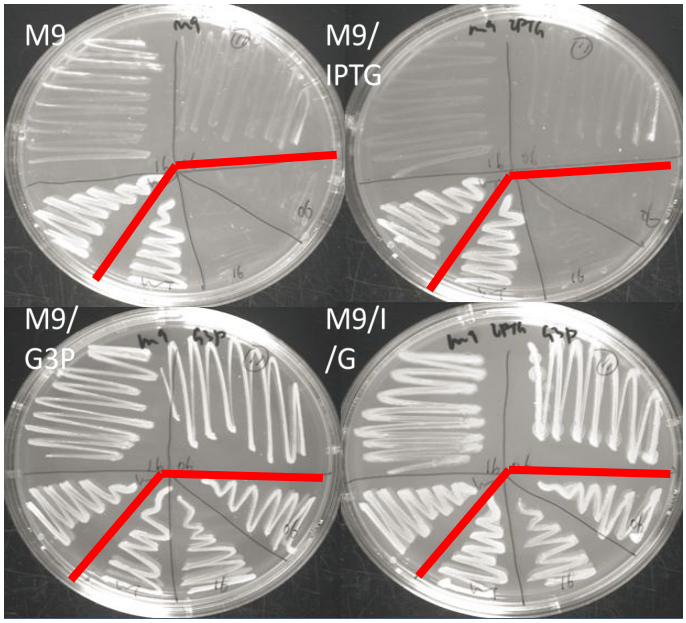

S. coelicolor complementation result

pTH2571 (*S. coelicolor pap-pitH1* in pTRsc) complement (++). In this set, the wild type without the plasmid is omitted.

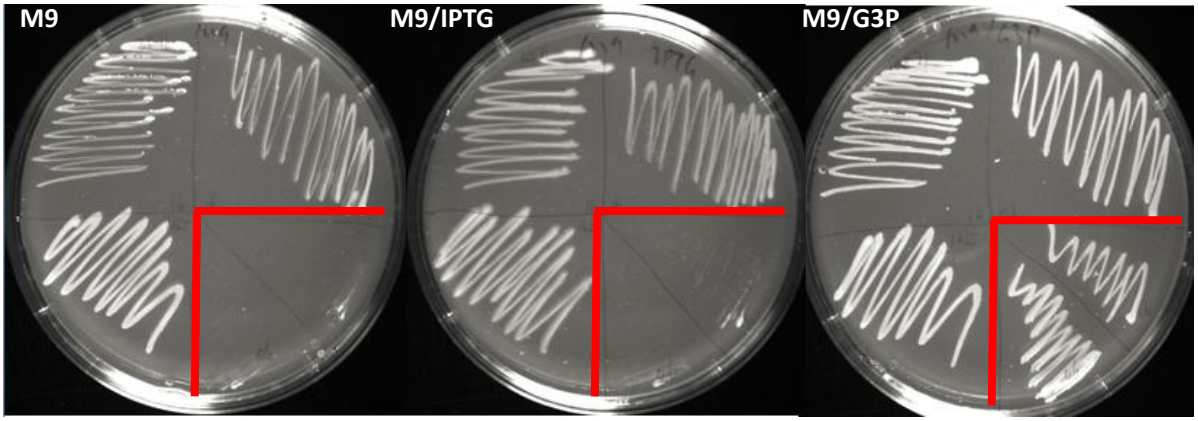

pTH2631 (*S. coelicoloe pitH1* in pTRsc) complement on M9, but is lethal on M9/IPTG (++)

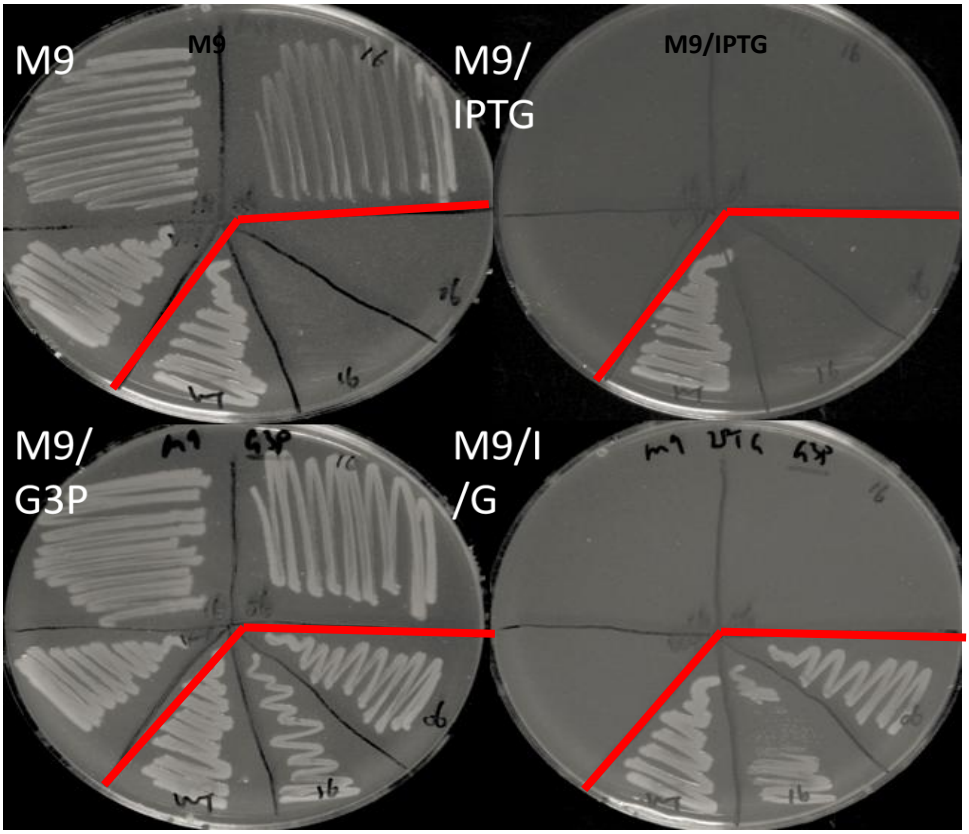

pTH2864 (*S. coelicolor pap* in pUC119) didn't complement (-)

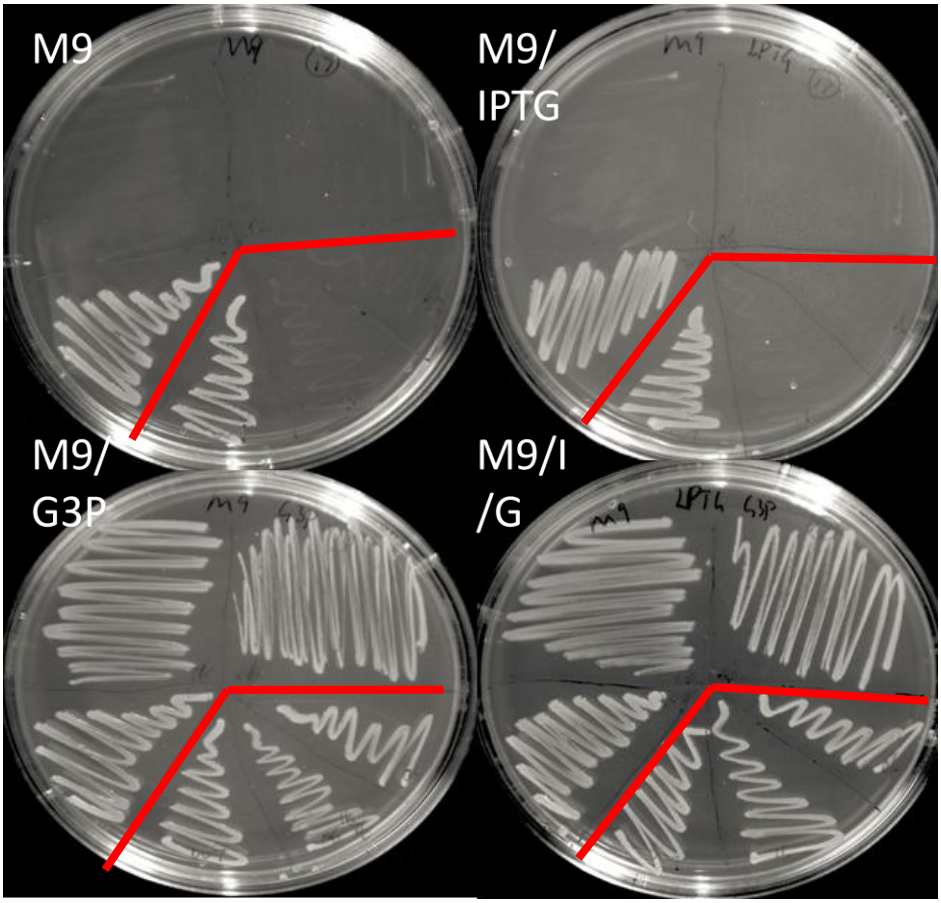

pTH2864 (*S. coelicolor pap* in pUC119) **plus** pTH2631 (*pitH1* in pTRsc) complemented on M9/IPTG (++).

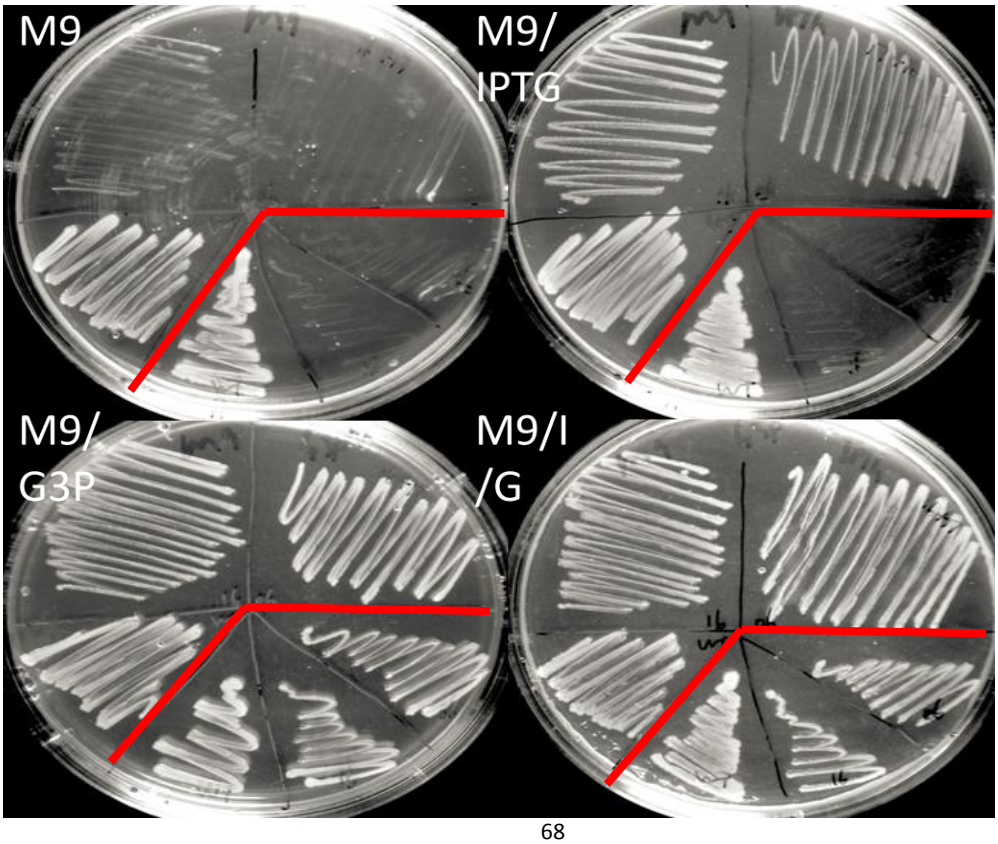

pTRsc vector: complemented to a low degree (+/-):

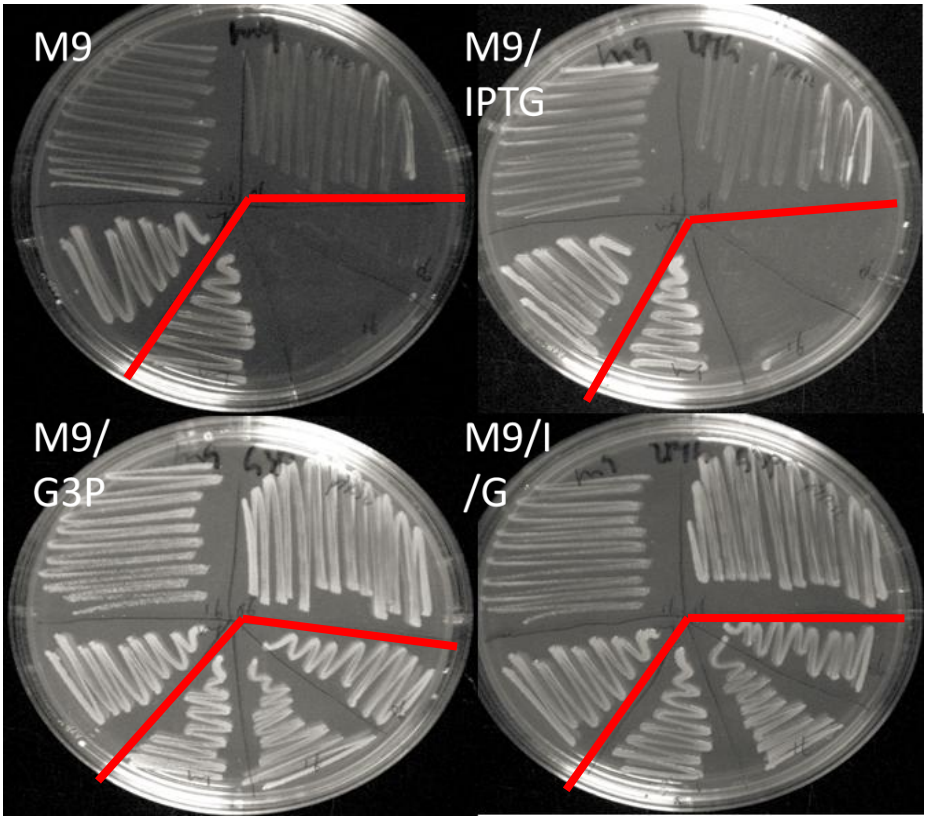

Figure 17. Complementation results of the clones for the *E. coli* Pi uptake mutants MT2006 and MT2016.

A

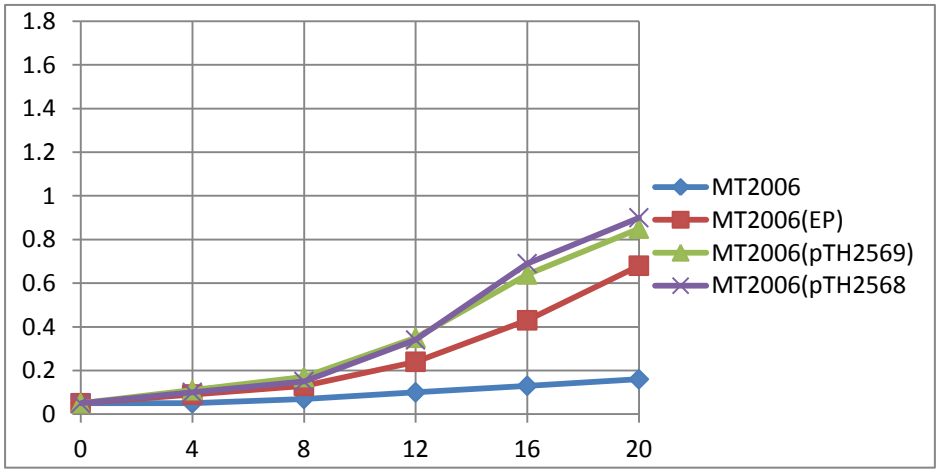

B

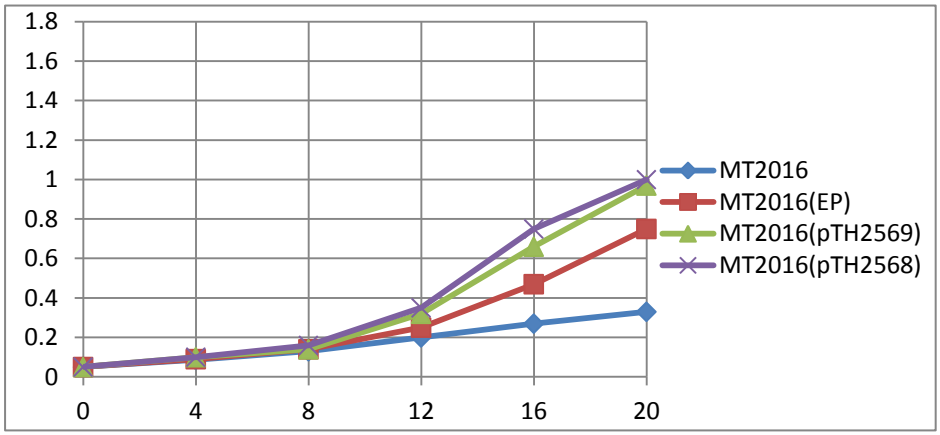
1.8
1.6
1.4
1.2
1
0.8
0.6
0.4
0.2
0
0
4
8
12
16
20
MT2016
MT2016(EP)
MT2016(pTH2569)
MT2016(pTH2568)

C

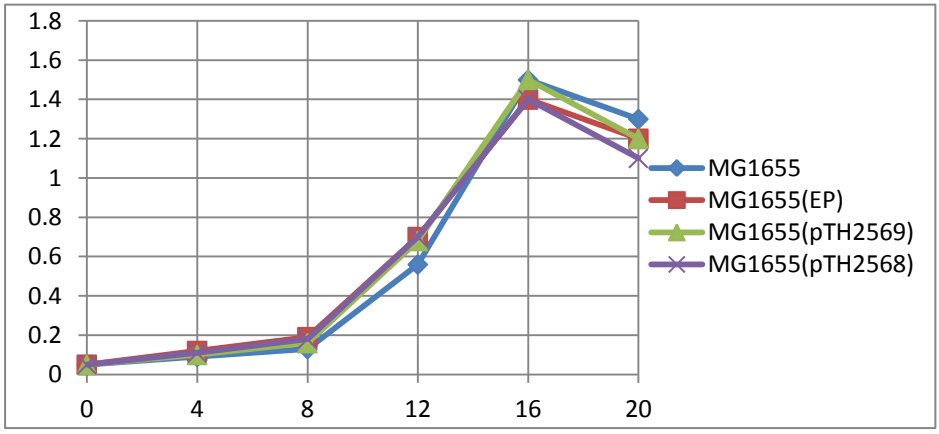
1.8
1.6
1.4
1.2
1
0.8
0.6
0.4
0.2
0
0
4
8
12
16
20
MG1655
MG1655(EP)
MG1655(pTH2569)
MG1655(pTH2568)

D

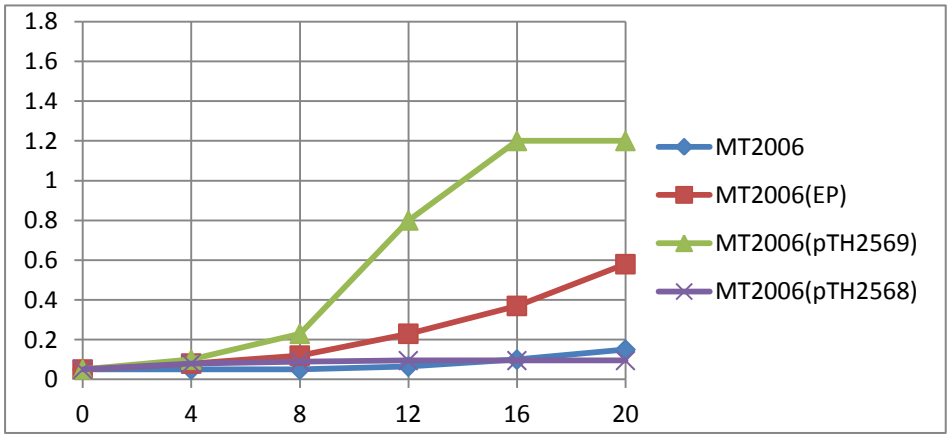
1.8
1.6
1.4
1.2
1
0.8
0.6
0.4
0.2
0
0
4
8
12
16
20
MT2006
MT2006(EP)
MT2006(pTH2569)
MT2006(pTH2568)

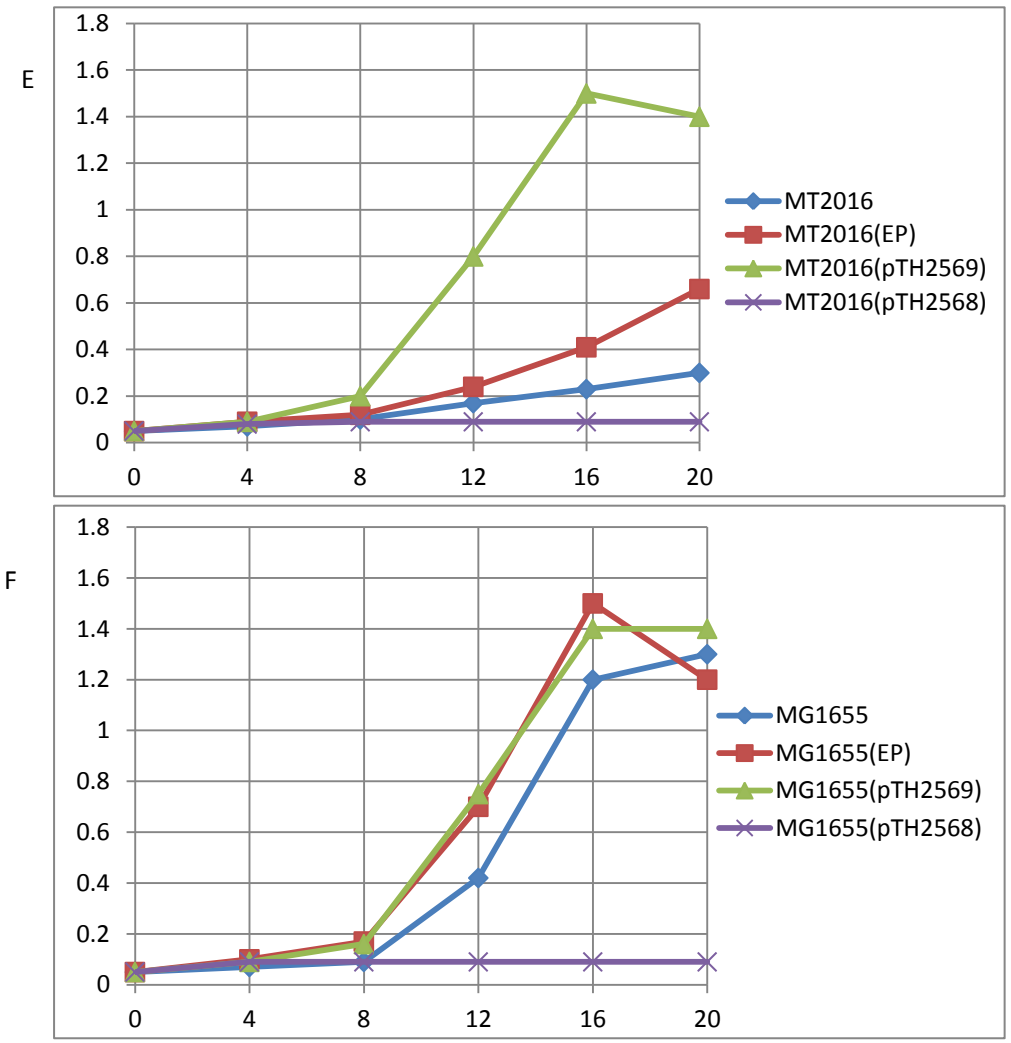

Figure 18. Growth curves showing the complementing effect of pTH2569 (*S. meliloti pap-pit* in pTRsc) and pTH2568 (*S. meliloti pit* in pTRsc) compared to pTRsc vector. In each chart, 4 cultures involved are listed in the right margin and represented by different colors. The 4 cultures are the host and the host carrying the empty plasmid (EP) pTRsc, pTH2568 and pTH259. The X-axis is the hours of incubation and y-axis is the optical density value at specific time point. Charts A, B and C are the strains grown in M9 media. Charts D, E and F are the same strains grown in M9 supplemented with 0.5 mM IPTG. pTH2569 appears to complement the host mutants when IPTG is present compared to EP whereas pTH2568 seems to inhibit the host mutants when IPTG is present.

A

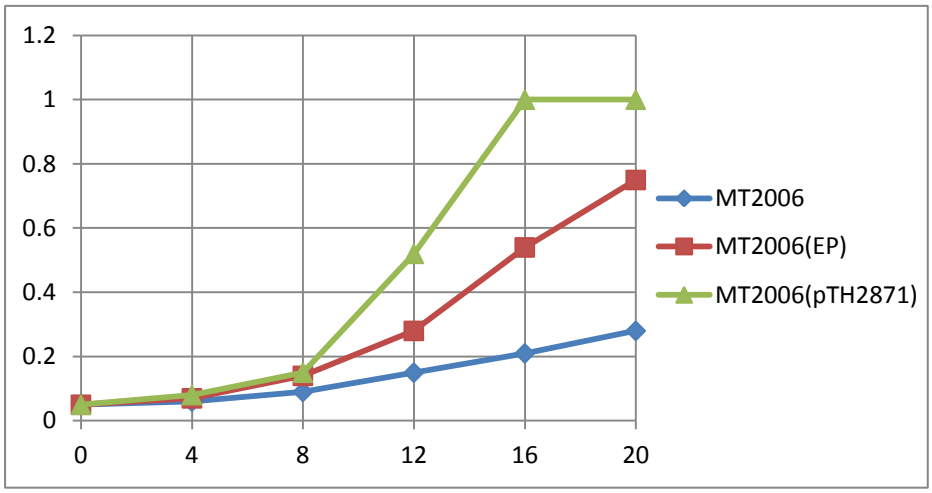
1.2
1
0.8
0.6
0.4
0.2
0
0
4
8
12
16
20
MT2006
MT2006(EP)
MT2006(pTH2871)

B

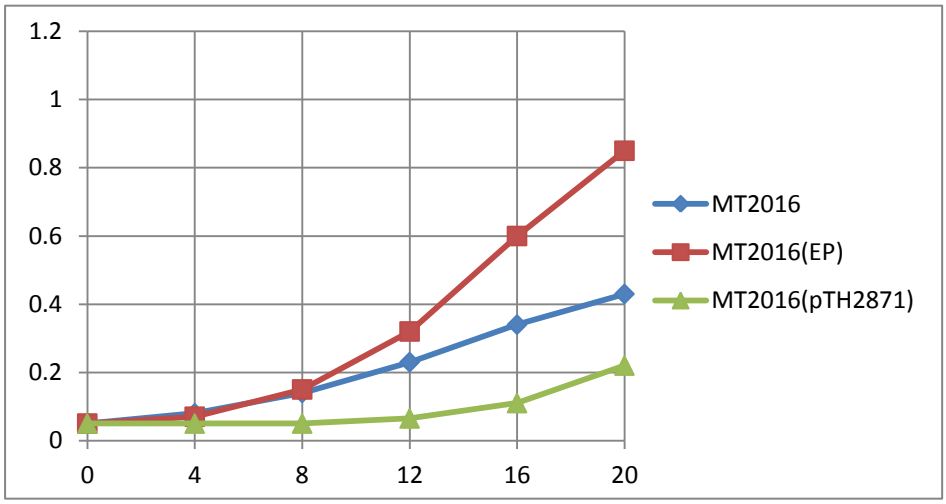
1.2
1
0.8
0.6
0.4
0.2
0
0
4
8
12
16
20
MT2016
MT2016(EP)
MT2016(pTH2871)

C

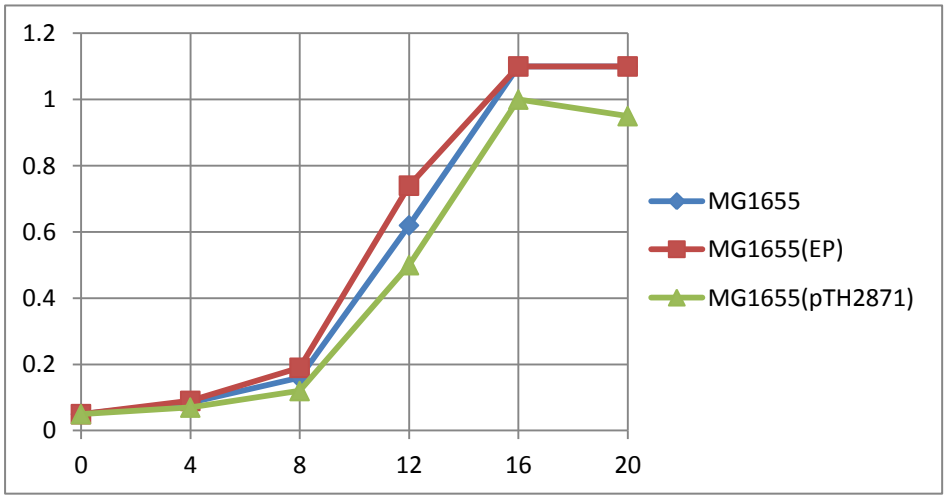
1.2
1
0.8
0.6
0.4
0.2
0
0
4
8
12
16
20
MG1655
MG1655(EP)
MG1655(pTH2871)

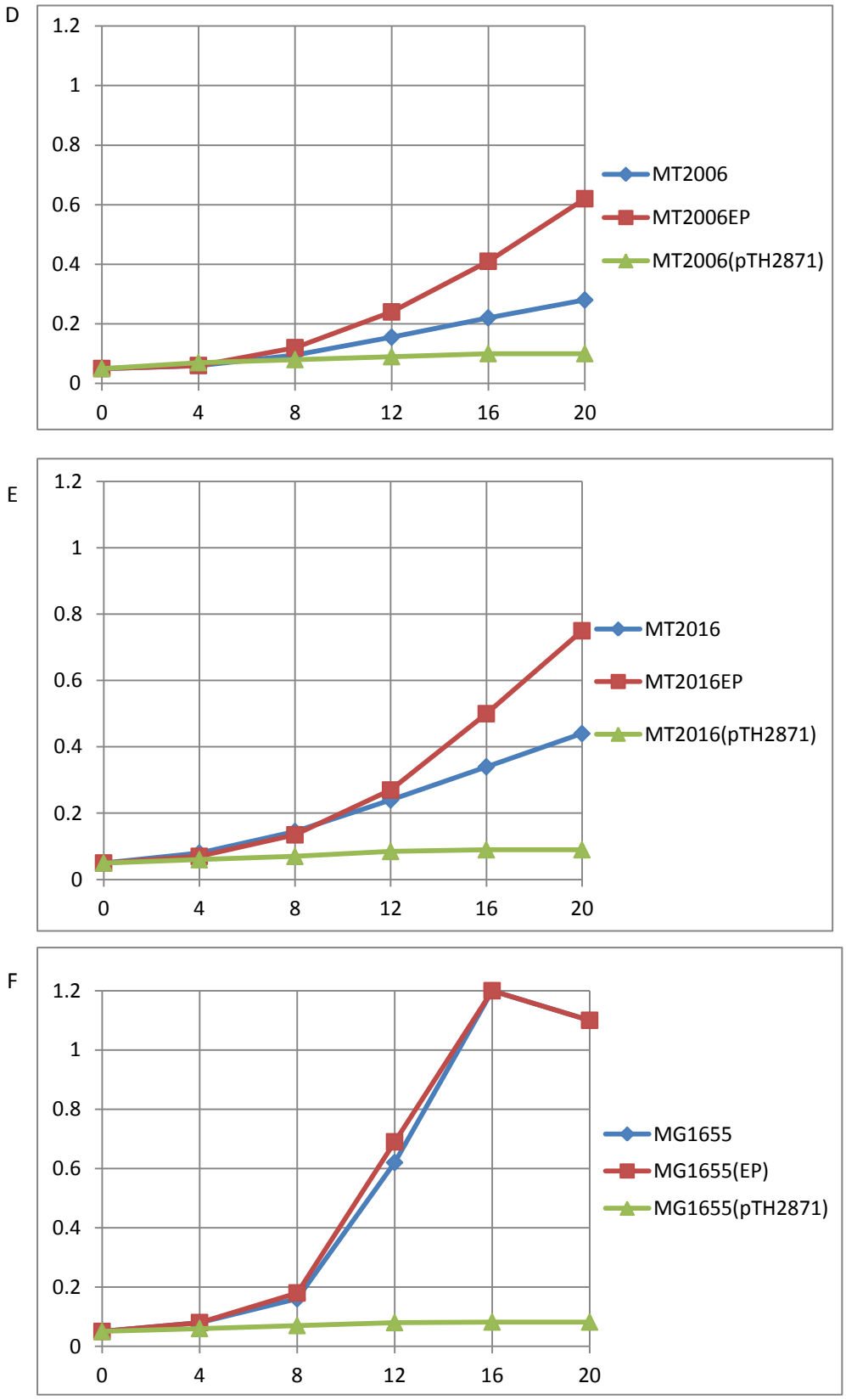

Figure 19. Growth curves showing the complementing effect of pTH2871 (*S. oneidensis pap-pit* in pTRsc) compared to pTRsc vector. In each chart, 3 cultures involved are listed in the right margin and represented by different colors. The 3 cultures are the host cell, the same host carrying the

empty plasmid (EP) pTRsc and pTH2871 separately. The X-axis is the hours of incubation and y-axis is the optical density value at specific time point. Charts A, B and C are the strains grown in M9 media. Charts D, E and F are the same strains grown in M9 supplemented with 0.5 mM IPTG. It can be see that pTH2871 inhibited the host cell growth when IPTG is present although it complemented MT2006 in M9.

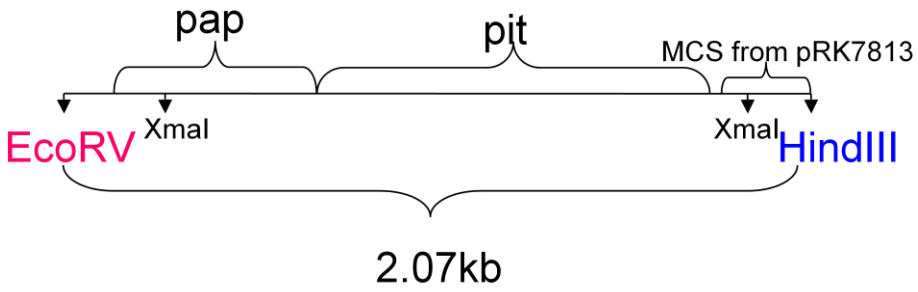

Figure 20. A 2.07kb fragment obtained by digesting pTH348 with *EcoRV* and *HindIII* and subcloned into pUC118 via *SmaI* and *HindIII* to prepare the plasmid pTH2825. The backbone of pTH348 is pRK7813 and a small fragment (~50bp) from pRK7813 was also cut out and cloned into pUC118.

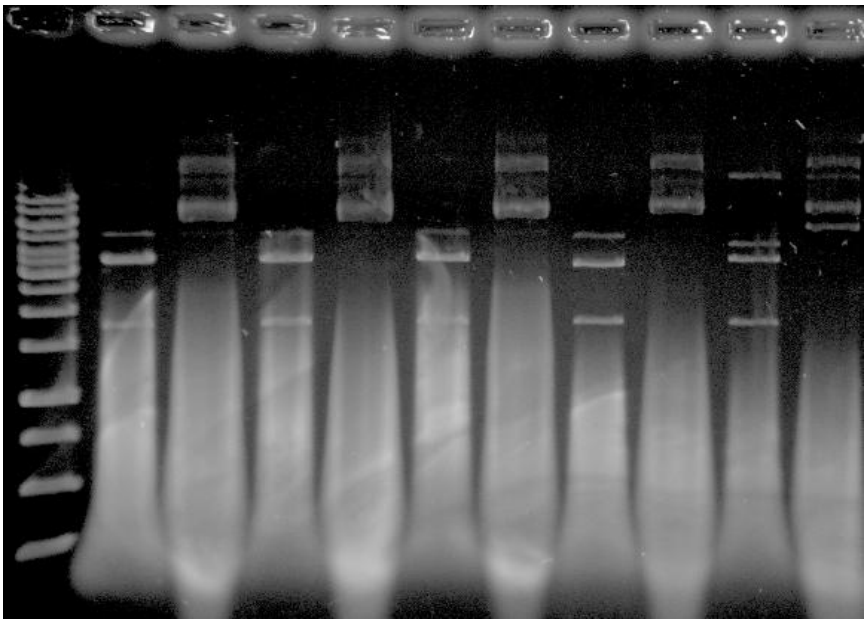

Figure 21. Double digestion result of the possible positive clones with *XmaI* showing the 1.8kb *XmaI-XmaI* fragment. The smear was RNA because RNAse was forgotten to be added before digestion.

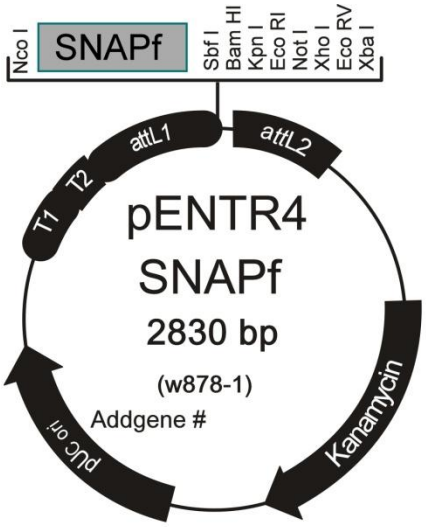

Comments for pENTR4 SNAPf 2830 nucleotides

rrnB T1 transcription termination sequence: bases 106-149
rrnB T2 transcription termination sequence: bases 281-308
attL1: bases 358-457 (complementary strand)
SNAPf ORF: 463-1008
Multiple cloning site (MCS): bases 1009-1059
attL2: bases 1059-1159
Kanamycin resistance gene: bases 1281-2090
pUC origin: bases 2200-2827

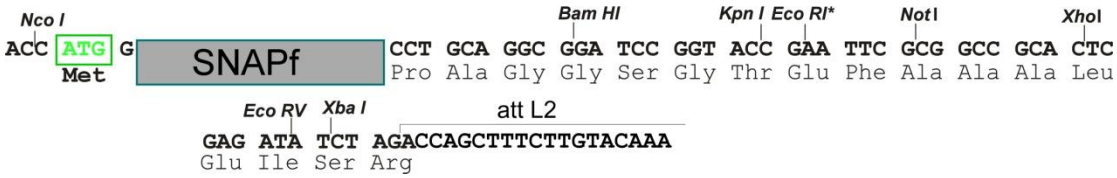

Figure 22. Map and comments for pENTR4 SNAPf which is the source of SNAP DNA. http://www.addgene.org/29652/

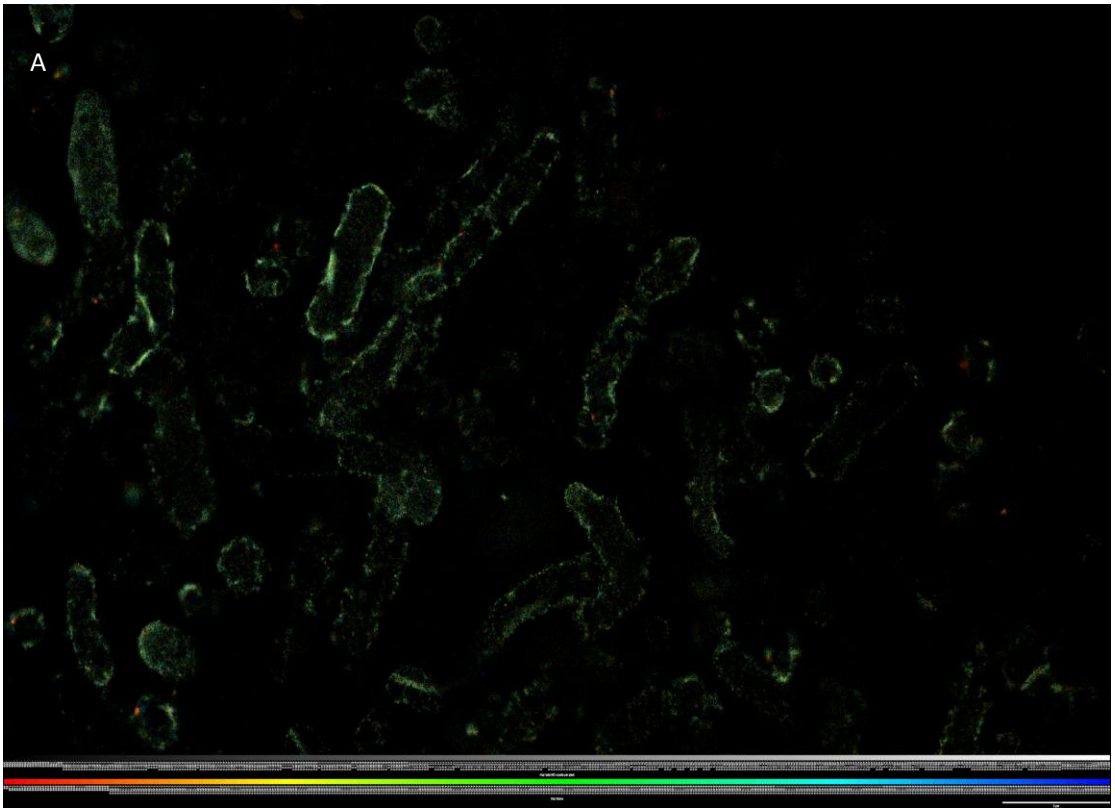
A

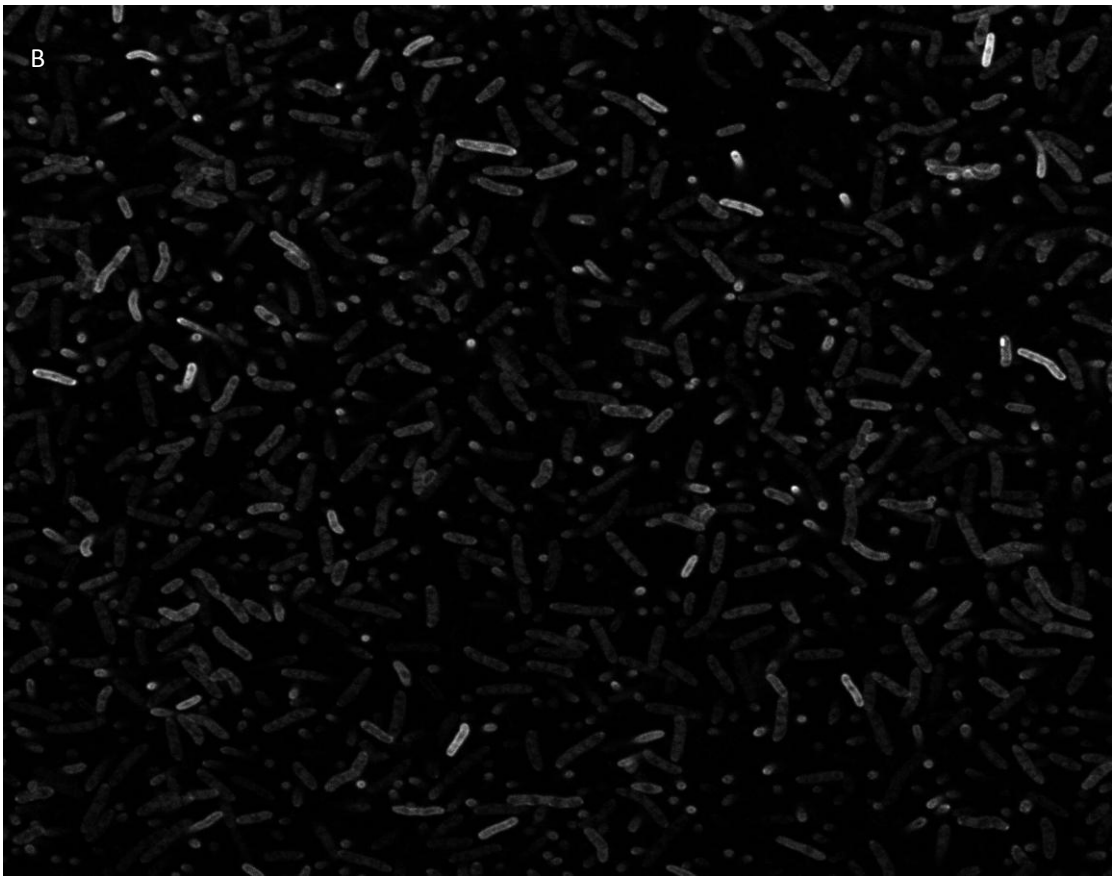
B


C

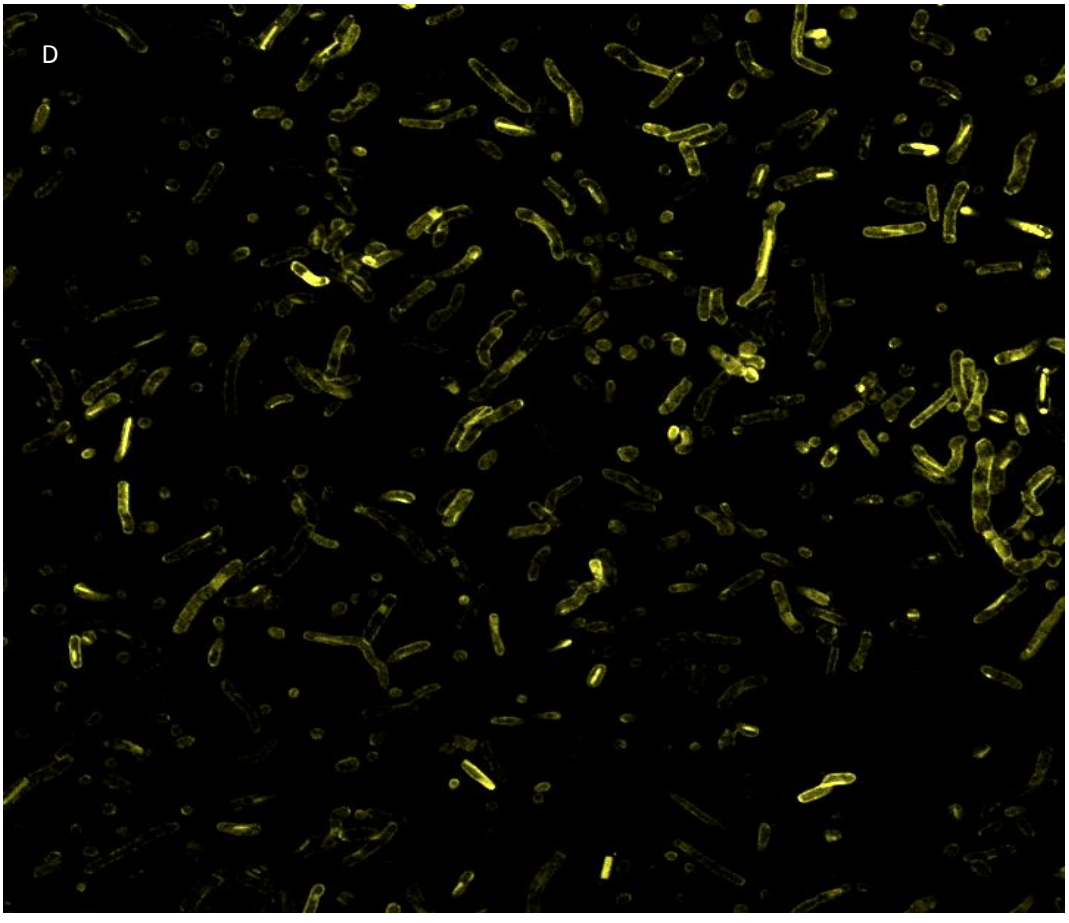
D

Figure 23. Microscopic pictures showing *E. coli* strains carrying pTH2868 which expresses SNAP-Pap-Pit and complement the *E. coli* Pi uptake mutants. A is the super-resolution fluorescent microscope image of MT2016 carrying pTH2868. The rest are confocal microscope images. B and C are MG1655 carrying pTH2868 and D is MT2016 carrying pTH2868.

Table 6. Primers employed for the preparation of the plasmids in this study

Clones	**Description**	**Primers employed**
pTH2824	*S. meliloti pap-pit* with 500bp upstream and downstream region of *pap-pit* cloned into pUCP30T	pap 500-up F & pit 500-dn R
pTH2826	*S.meliloti pap-pit* cloned into pUC119 via *HindIII* and *XbaI*	Smel pap-F & Smel pit-R
pTH2827	*S. meliloti pap-pit* cloned in pRK7813 via *HindIII* and *BamHI*	Smel pap-F& Smel RK-R
pTH2828	*S.meliloti pap-pit* cloned into pMW119 via *HindIII* and *XbaI*	Smel pap-F & Smel pit-R
pTH2829	*S. meliloti pit* and cloned into pMW119 via *HindIII* and *XbaI*	Smel pit-F and Smel pit-R
pTH2863	*S. oneidensis pap* cloned in pTRsc via *PacI and HindIII*	SonePapTR-F & SonePap TR-R
pTH2864	*S. coelicolor pap* cloned into pUC119 via *HindIII and XbaI*	Scoe pap-F & Scoe pap-R
pTH2871	*S. oneidensis pap-pit* cloned in pTRsc via *PacI* and *HindIII*	SonePapTr F* & SonePit Tr R
pTH2872	*S. oneidensis pap-pit* cloned in pMW119 via *HindIII* and *XmaI*	2 Sone pap-F & Sone pit-R
pTH2873	*S. oneidensis pap-pit* cloned into pMW119 via *HindIII and XmaI*	2 Sone Pit-F & Sone Pit-R
pTH2867	pENTR4 SNAPf carrying pap-pit fragment between *KpnI* and *XbaI* with pap start codon ATG removed	2 Mpap SNAP-F & Smel pit-R
pTH2868	SNAP-*pap-pit* PCR amplified from pTH2867 and cloned into pUCP30T between *XbaI* and *HindIII*	2 SNAP-F & pENTR4 pit R
pTH2869	200bp upstream of *pap* was PCR amplified and cloned into pTH2868 between SacI and XbaI upstream of SNAP-pap-pit	prom pap-F & 2 prom pap-R

*Please note that SonePap TR-F and SonePapTr-F are different primers.

Table 7. Sequences of the primers employed

Primers	Sequence	References
SmeI pap-F	GTA AGC TTT GGA TGG ATC GCT G**AT G**	This study
SmeI pit-R	GTT CTA GAA AAG CG**T CA**G GCG ACG	This study
SmeI RK-R	GTG GAT CCA AAG CG**T CA**G GCG ACG	This study
SmeI pit-F	GTA AGC TTT G**AT G**GA TGC GAC GCT C	This study
2 Sone pap-F	GTA AGC TTA ATA GGT AAA CGG CA**A TG**	This study
2 Sone Pit-F	GTA AGC TTA TGG TTG ATG CAG GT**A TG**G	This study
Sone Pit-R	GTC CCG GGC CAG TTT TGT GCT TCT **TTA** GT	This study
SonePapTr F*	GCT TAA TTA AAA TAG GTA AAC GGC A**AT G**	This study
SonePitTr R	GTA AGC TTC CAG TTT TGT GCT TCT **TT**	This study
SonePapTR-F	GCT TAA TTA AAT AGG TAA ACG GCA **ATG** CCA G	This study
SonePapTR-R	GTA AGC TTC CTG CAT CAA CCA TAT TGA TAC C	This study
Scoe pap-F	GCA AGC TT**G TG**C GCT TTC GTC TGA C	This study
Scoe pap-R	CAT CTA GAC **TCA** GGA CTC CTT GAC GG	This study
pap 500-up F	GTT CTA GAC CGA TCT CCA CCG ACC	This study
pit 500-dn R	GTA AGC TTC TTT CGA CGT CGA TCT CG	This study
2 Mpap SNAP-F**	CCG GTA CCC TCG GCC TGT TTC GCA AG	This study
2 SNAP-F***	GCT CTA GAC C**AT G**GA CAA AGA CTG CG	This study
pENTR4 pit R	GTA AGC TTA AAG CG**T CA**G GCG ACG	This study
prom pap-F	GAG AGC TCA TGA AAG CCC GGC CAAG	This study
2 prom pap-R	GCT CTA GAC AGC GAT CCA TCC AAC TGTC	This study
orfA F	CCT TAA TTA AC**A TG**C TCG GCC TGT TTC GCA AGC TC	Zaheer
smpit R	CGT AAG CTT **TCA** GGC GAC GAG GTC CGC GGC G	Zaheer
Scoeli F	CCT TAA TTA AC**A TG**C GCT TTC GTC TGA CCC CCA GGG	Zaheer
Scoeli R	CGT AAG CTT CTA CAG GAC CGC CAG GT**T CA**C GAT CC	Zaheer
pitH-F2	CCT TAA TTA AC**A TG**G ACA CCT TTG CTC TGG TCG TGA CC	Zaheer

The underlined sequences are restriction sites. The nucleotides in bold are start codons or stop codons.

* SonePapTr-F is a different primer than SonePap TR-F

***pap* start codon is not included for SNAP fusion

***The ATG here is the start codon of SNAP instead of Pap

The following figures are the maps of the vectors used for cloning.

A. pUC119 (Vieira et al, 1987)

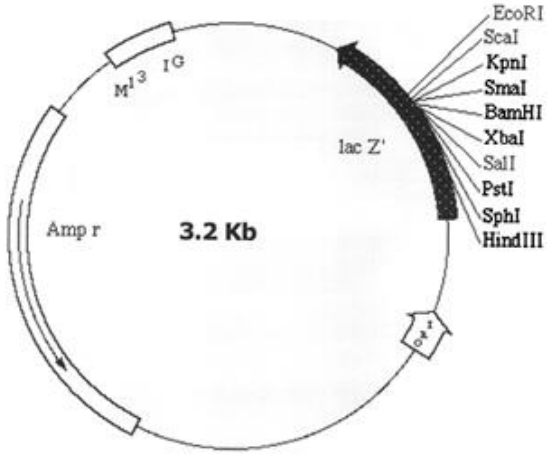

Map of pUC119

http://www.rci.rutgers.edu/~microlab/CLASSINFO/IMAGESCI/plasmid%20maps.htm

B. pUC118 is pUC119 with reverted MCS region

C. pTRsc (C. Baron, unpublished)

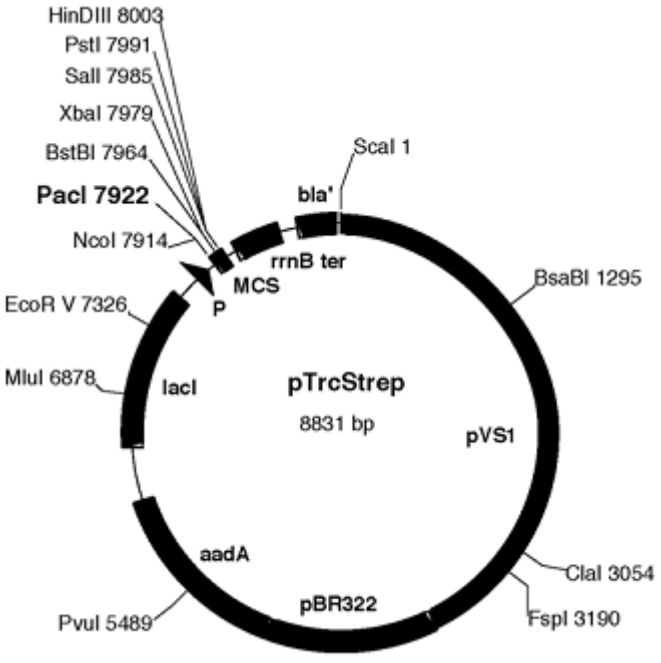

D. pMW119 (A gift from Dr. Kuroda)

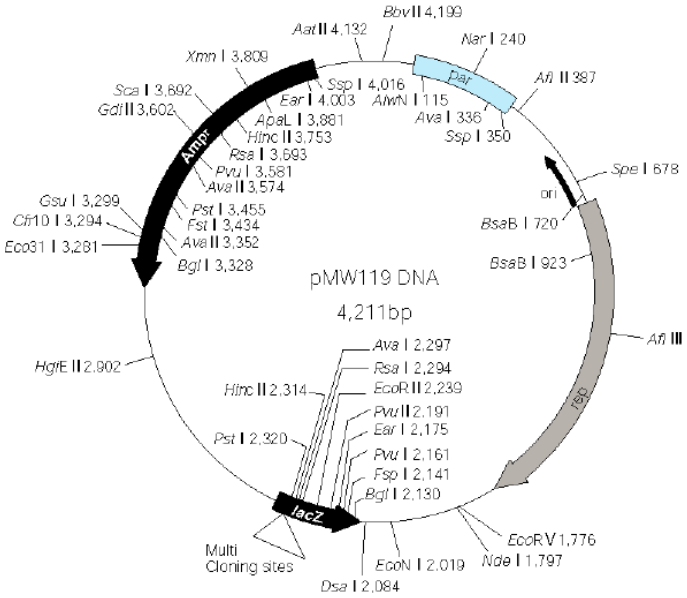

The multiple cloning sites are the same as in pUC119.

E. pUCP30T (Schweizer 1996)

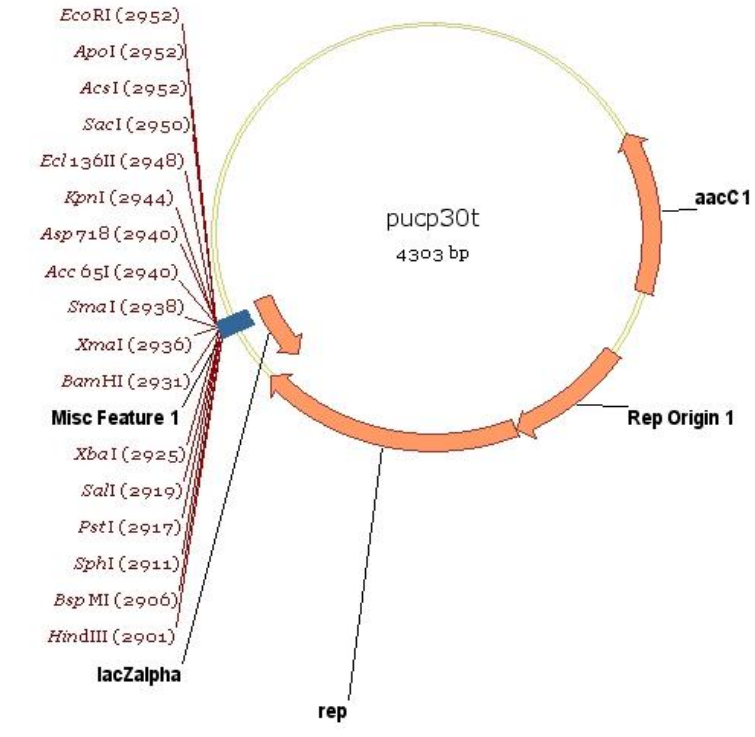

F. pRK7813 (Jones and Gutterson 1987)

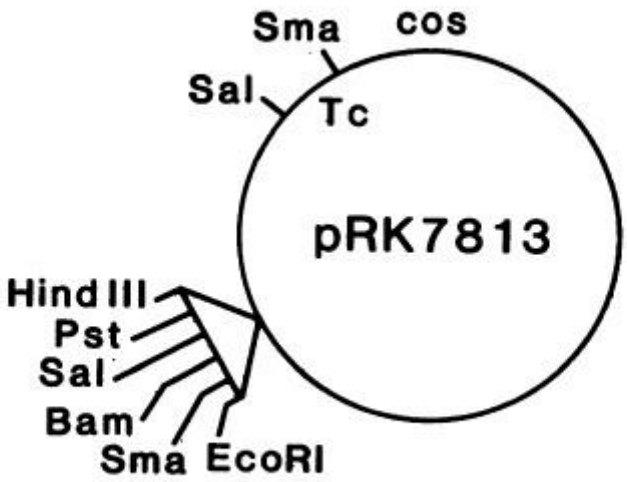

Figure 24. Maps of the vectors used for the preparation of the plasmids involved in the complementation experiments and *pap-pit* deletion.